THERMOMECHANICAL CHARCTERISTICS OF NITINOL

John Michael Johnson

NAVAL POSTGRADUATE SCHOOL
Monterey, California

THESIS

THERMOMECHANICAL CHARACTERISTICS
OF NITINOL

by

John Michael Johnson

March 1975

Thesis Advisor: G. R. Edwards

UNCLASSIFIED

SECURITY CLASSIFICATION OF THIS PAGE (When Data Entered)

REPORT DOCUMENTATION PAGE		READ INSTRUCTIONS BEFORE COMPLETING FORM
1. REPORT NUMBER	2. GOVT ACCESSION NO.	3. RECIPIENT'S CATALOG NUMBER
4. TITLE (and Subtitle) Thermomechanical Characteristics of Nitinol		5. TYPE OF REPORT & PERIOD COVERED Master's Thesis March 1975 6. PERFORMING ORG. REPORT NUMBER
7. AUTHOR(s) John Michael Johnson		8. CONTRACT OR GRANT NUMBER(s)
9. PERFORMING ORGANIZATION NAME AND ADDRESS Naval Postgraduate School Monterey, California 93940		10. PROGRAM ELEMENT, PROJECT, TASK AREA & WORK UNIT NUMBERS
11. CONTROLLING OFFICE NAME AND ADDRESS Naval Postgraduate School Monterey, California 93940		12. REPORT DATE March 1975 13. NUMBER OF PAGES 67
14. MONITORING AGENCY NAME & ADDRESS(if different from Controlling Office) Naval Postgraduate School Monterey, California 93940		15. SECURITY CLASS. (of this report) Unclassified 15a. DECLASSIFICATION/DOWNGRADING SCHEDULE

16. DISTRIBUTION STATEMENT (of this Report)

Approved for public release; distribution unlimited.

17. DISTRIBUTION STATEMENT (of the abstract entered in Block 20, if different from Report)

18. SUPPLEMENTARY NOTES

19. KEY WORDS (Continue on reverse side if necessary and identify by block number)

Nitinol
Stress relaxation
Flow stress
Reversion stress

20. ABSTRACT (Continue on reverse side if necessary and identify by block number)

The flow stress of a common shape memory alloy, a particular alloy of nitinol, is investigated and presented as a function of temperature and strain. The reversion stress, that stress necessary to maintain a constant strain as a result of a martensitic phase transforming to the parent phase, is presented as a function of temperature and amount of pre-strain. This reversion stress is demonstrated to approximate,

DD FORM 1 JAN 73 1473 EDITION OF 1 NOV 65 IS OBSOLETE
S/N 0102-014-6601 |
(Page 1)

UNCLASSIFIED

SECURITY CLASSIFICATION OF THIS PAGE (When Data Entered)

during the cooling process, the flow stress. The stability of the reversion stress is investigated and is presented as a function of time at 220 C. A model of a shipboard device utilizing a shape memory alloy is constructed and studied to compare with pure tensile data.

Thermomechanical Characteristics of Nitinol

by

John Michael Johnson
Lieutenant, United States Navy
B.S., Pennsylvania State University, 1967

Submitted in partial fulfillment of the
requirements for the degree of

MASTER OF SCIENCE IN MECHANICAL ENGINEERING

from the

NAVAL POSTGRADUATE SCHOOL
March 1975

ABSTRACT

The flow stress of a common shape memory alloy, a particular alloy of nitinol is investigated and presented as a function of temperature and strain. The reversion stress, that stress necessary to maintain a constant strain as a result of a martensitic phase transforming to the parent phase, is presented as a function of temperature and amount of pre-strain. This reversion stress is demonstrated to approximate, during the cooling process, the flow stress. The stability of the reversion stress is investigated and is presented as a function of time at 220 C. A model of a shipboard device utilizing a shape memory alloy is constructed and studied to compare with pure tensile data.

TABLE OF CONTENTS

LIST OF TABLES

LIST OF FIGURES

ACKNOWLEDGEMENTS

This study was a portion of an ongoing program supported by the Naval Weapons Laboratory, Dahlgren, Virginia.

The nitinol alloys used were provided by Raychem Corporation, Menlo Park, California. The assistance provided by Dr. Jack Harrison was greatly appreciated.

I. INTRODUCTION

The phenomenon of thermoelastic martensitic reversion or shape memory effect (hereafter referred to as "SME") has recently been widely discussed, particularly as it applies to the nitinol alloys. [Ref. 1,2,3] To date most works on SME deal with mechanistic and phenomenological interpretations, although there are numerous exceptions. Cross, et al, [Ref. 4] collected a large quantity of physical data to provide a background for a quantitative understanding of SME. Tong and Wayman [Ref. 5] discussed the thermodynamic considerations of a solid state engine based on SME. Such [Ref. 6] presented some characterizations of the reversion stress for nitinol.

The purpose of the present study was to further characterize the reversion stress with the particular goal of supporting the application of nitinol as a shipboard material. Demands placed upon shipboard materials are many and varied depending upon their specific application. There is a specific requirement for a material which is (1) corrosion resistant, (2) able to withstand heavy wear, and (3) able to withstand high shock loads. A high grade ceramic such as pure alumina (Al_2O_3) fulfills the first two requirements, and if it were placed in a high compressive pre-strain, it could easily

fulfill the third requirement. For certain geometries, a shape memory material could easily be used to pre-strain the ceramic. Such a composite body (SME material plus ceramic) could easily fulfill the three requirements and at the same time be practical in the sense of manufacture and procurement.

Development of such a composite body carries a prerequisite of first having a substantial understanding of the reversion stress in the shape memory material, and the increase of that understanding was the intent of this investigation.

The thermoelastic martensitic reversion is defined when a material, apparently plastically deformed, reverts to its original shape on heating to a temperature somewhat above the deformation temperature. It has been reported in numerous materials, but has been popularized by its discovery in near equiatomic nickel-titanium (nitinol).

There are several mechanisms by which the SME may occur. These will be discussed below after first defining several terms important to the study.

Figure 1 shows a thermal hysteresis curve for nitinol at a given stress level (usually at zero stress). The point T_o is the thermodynamic equilibrium temperature at which the chemical free energy of martensite is equal to that of the high temperature phase. M_s is the temperature at which the formation of thermal martensite will begin to occur, and A_s is the temperature at which the reversion to the high temperature phase will begin to occur.

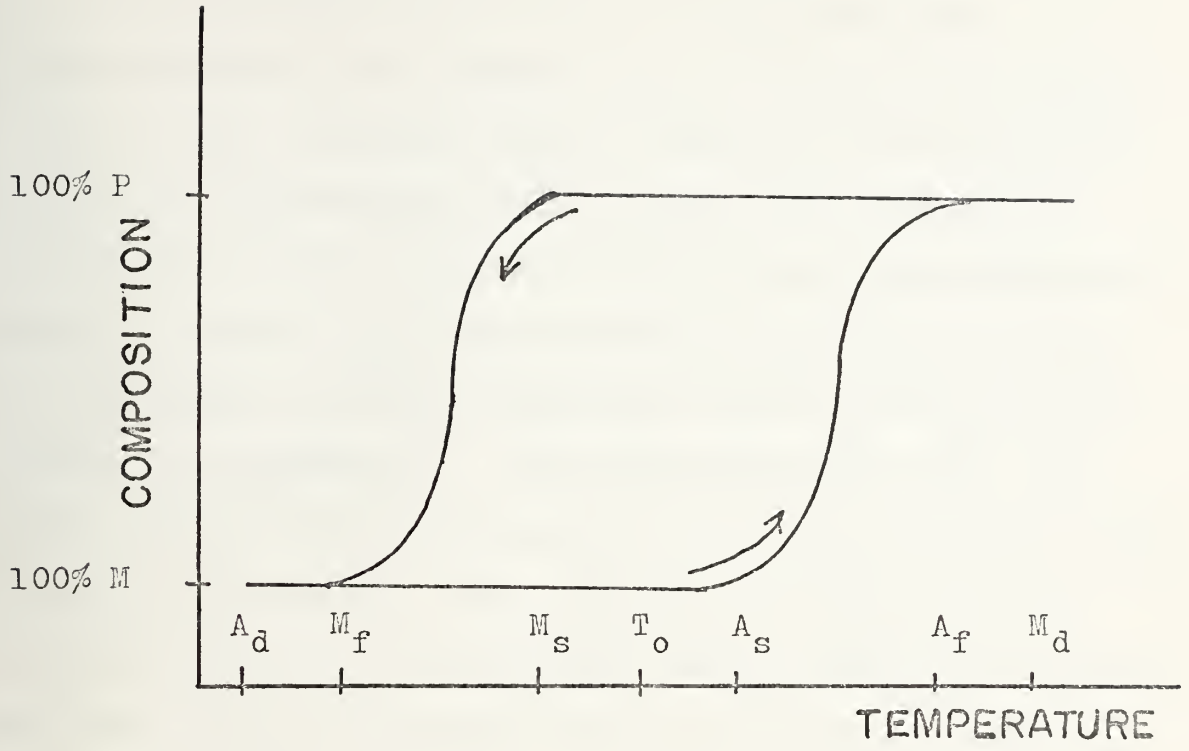

Figure 1. The thermal hysteresis curve for the thermal phase transformations in nitinol.

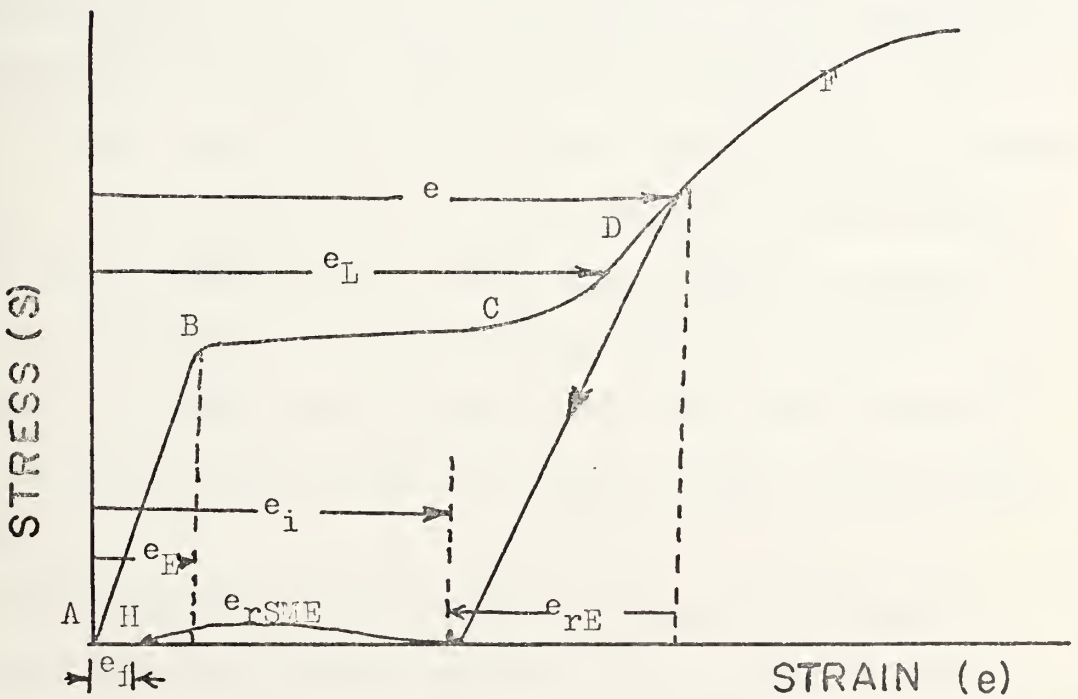

Figure 2. Typical stress/strain curve for nitinol showing important points.

M_f and A_f are the temperatures at which the phase transformations are complete. M_d is the maximum temperature at which martensite may be formed by the deformation of the high temperature phase. Above this temperature, strain will result in plastic flow of the high temperature phase. Likewise, A_d is the minimum temperature at which the martensite to high temperature phase reaction can be induced by deformation. Tong and Wayman [Ref. 7] have shown that if the intervals M_s to A_f and A_s to M_f are small, T_o may be approximated as $T_o=\frac{1}{2}(M_s+A_f)$. They have also defined a point T_o' which, if the before mentioned intervals are small, may be approximated $T_o' =\frac{1}{2}(A_s+M_f)$. T_o and T_o' are then the end points in a temperature scale for thermoelastic equilibrium. All these points are functions of alloying and are of prime importance to this investigation. They need not lie in the order shown in Figure 1. The loop could be very broad and have M_s less than A_d, and A_s greater than M_d. In this case, the stress assisted transformation product would remain stable after the stress is removed. However, the general case for SME materials is as shown in Figure 1. Under these conditions, the stress assisted transformation product need not remain stable after stress removal.

Figure 2 shows the stress/strain curve for nitinol below A_s. The total strain applied is e; e_E is the true elastic strain (as opposed to pseudoelastic), and e_i is

the initial martensitic strain which is produced by the transformation $A \xrightarrow{S} M(d)'$ and/or $M(t) \xrightarrow{S} M(d)''$, where M(d) is the stress-induced martensite and M(t) is the athermal martensite. e_{rE} is the immediate (elastic) reversion strain; e_{rsme} is the heat activated (SME) reversion strain; $e_r = e_{rE} + e_{rsme}$. e_f is the residual strain after heating above A_f, $e_f = e_i - e_r$. e_L is the strain limit for $e_f = 0$; that is, it is the strain limit for "complete" reversion.

It has been shown [Refs. 1,2, and 3] that alloy systems which demonstrate SME often have a BCC structure for a high temperature phase and undergo a low hysteresis martensitic transformation on cooling, and this transformation must be thermoelastic. Deformation of the SME alloy in the martensitic phase must result via internal twinning of the martensite plates since deformation by slip is irreversible. Transmission electron microscopy has shown the presence of twinned martensites in SME alloys. These twins are quasi-reversible, so that the reverse transformation and the detwinning of the martensite presumably allows the nearly reversible SME to occur. Wasilewski [Ref. 2] has shown nine slightly different mechanisms by which this may occur.

Referring to Figure 2, the general mechanism may be described. The exact procedure will vary depending on T_d (the deformation temperature) and e (the maximum applied strain). AB is simple elastic strain of the athermal

martensite. BC represents transformation of M(t) to M(d). CD represents internal twinning of the stress induced martensite. DF is the plastic deformation of the twinned martensite. At F the load is removed and the elastic strain is recovered back to G. If the specimen is then heated to above A_f, the transformation $M(d) \longrightarrow A$ occurs and e_{rsme} is recovered. In general, e_f is equal to the amount of strain by which e exceeds e_L, providing $e-e_L$ is small. If, however, the strain is prevented from dropping below some fixed point during heating, a reversion stress (S_r) will develop. e_{rfree} is the unconstrained portion of the reversion strain, and e_{rcon} is the constrained portion. If the material is mechanically constrained at e_i throughout the heating process, it is said to be fully constrained and the maximum reversion stress will develop. Whether or not this stress will relax in time has much engineering significance and is one aspect to which this project is directed.

Stress relaxation in the classical sense occurs when the elastic strain energy which is stored in the specimen and tensile device plastically deforms the specimen. If a specimen is deformed in a stiff tensile machine by moving the crosshead, and the crosshead is then stopped, the specimen will continue to deform under a decreasing stress and a decreasing strain rate due to the motion of mobile dislocations. In this classical case $dS/dt = -S/\lambda$, where

λ is a material constant "relaxation time." The stress is that which is necessary to cause the movement of dislocations, and hence some non-elastic deformation of the material. However, in a SME material, the stress is internally developed via the reverse transformation and the constraints on strain. The relationship between any relaxation of this reversion stress and any microstructural change which might occur is not yet fully understood.

A difficulty in investingating relaxation of reversion stress is the problem presented by the necessary temperature change. This temperature change causes thermal stress and strain not only in the specimen, but more significantly in the rig. This problem was circumvented by means of a device which is described under experimental procedure. To date only one stress relaxation investigation of an SME material has been reported [Ref. 6], and only one report of a stress relaxation test of any material at varying temperatures has been found [Ref. 8].

II. AREAS OF STUDY

A. GOALS

The ultimate goal of this project was to characterize the stability of the reversion stress in terms of parameters important to the fabrication and utilization of some composite device as described above. A starting point for this initial investigation was the determination of the optimum temperature and stress levels. To establish quantative data for use in engineering data would require a complete and separate study of every different alloy, and is beyond the scope of this investigation. Three different nitinol alloys were provided by Raychem Corporation. Table 1 shows an example of the wide variation in properties with only slight variation in alloying. Accordingly, the emphasis was placed on clearly understanding the reversion stress obtainable from one typical alloy. To accomplish this, four areas of study were chosen.

1. Characterization of flow stress as a function of temperature and strain.
2. Characterization of reversion stress as a function of temperature and strain.
3. Characterization of the stability of reversion stress as a function of time and temperature.

4. Observation of the reversion stress and its stability in a model device.

TABLE I

ALLOY	a/o Ti	a/o Ni	a/o Fe	a/o Al	Yield Strength Room Temperature
A	49.18	49.82	0	1.0	110 MPa (16 ksi)
B	49.50	49.50	1.0	0	345 MPa (50 ksi)
C	49.50	47.00	3.5	0	415 MPa (60 ksi)

B. FLOW STRESS

There are three basic reasons for the necessity of understanding flow stress. From a materials standpoint, any attempt to understand reversion stress without some grasp of the flow stress may prove to be lacking a proper foundation. Additionally, a comparison was drawn between reversion stress and flow stress with the intent that since it is sometimes more practical and possibly easier to characterize flow stress, if a relationship were known, the characterization of the reversion stress would be facilitated and/or supported. Finally, from an engineering standpoint, the efficiency of a device or system could be optimized by prestraining under conditions of minimum flow stress and reverting under conditions of maximum reversion stress. To obtain this flow stress data, stress/strain curves were

obtained at several temperatures, as described under experimental procedure, and these data were corrected for strain rate sensitivity.

C. REVERSION STRESS

Without the application of reversion stress, SME materials simply have the ability to return to their original shape. While this may be fascinating behavior, it has somewhat limited practical application, particularly in the sphere of engineering. It is then basic to any engineering study of SME to understand the reversion stress. Three questions are pertinent.

1. Under what conditions is the maximum reversion stress obtained?
2. What is the affect of change in the parameters on the reversion stress in the vicinity of this maximum point?
3. How is the maximum utilization of the reversion stress achieved?

There are many parameters which affect the magnitude of the reversion stress, e.g. temperature, time, pre-strain, unconstrained reversion strain, pre-strain temperature, and thermal history. Such [Ref. 6] discussed the effect of partial reversion of the initial strain, and the effect of cooling below M_d. Wasilewski [Ref. 2] discussed the

effects of pre-strain temperature. Cross, et al, [Ref. 4] discussed the effects of thermal history. With these parameters known, or at least discussed in the literature, the objective here was to map reversion stress as a function of temperature and pre-strain.

D. STRESS RELAXATION

Many applications of nitinol, particularly in the applications described above where a principal criteria is the resistance to wear, may involve high temperatures with respect to A_f and M_d. The stability of the reversion stress under such conditions is not well known. From an emperical standpoint, this aspect of SME has received very little investigation. This is a result of the fact that commercial engineering application of SME materials has been, to date, limited to hydraulic fittings manufactured by Raychem Corporation. From a mechanistic standpoint, the role of dislocations in the mechanical behavior of SME alloys has only recently begun to receive attention. Since stress relaxation is generally considered to be a result of dislocation mobility, the lack of theoretical or experimental data on the role played by dislocations in the behavior of SME alloys made any detailed study of stress relaxation difficult. This project utilized a purely emperical approach and limited the investigation to delineating possible temperature limits with respect to the stability of the reversion stress.

E. OBSERVATION OF MODEL TESTS

Any practical application of the recovery force available from a SME material will involve a stress state more complex than uniaxial tension. While uniaxial tensile test can provide the basic design information, model tests are often the most expedient way to approximate the material performance in its actual service environment. With this in mind, a model of a possible application was built and subjected to some, but not all, environments of interest. This was not done to establish stress levels which could be modeled to an actual structure, but to support or contradict the uniaxial tensile data.

III. EXPERIMENTAL PROCEDURE

A. ALLOY PREPARATION

Three nitinol alloys, described in Table I, were prepared and supplied courtesy of Raychem Corporation of Menlo Park, California. The following schedule was followed.

1. Alloys were melted by electron-beam into an ingot of 3.18 cm. diameter.
2. The ingot was hot swaged to a bar of 1.27 cm. diameter.
3. The bar was cold drawn with a pass schedule of 10% - 15% diameter reduction per pass to a final rod diameter of 0.2548 cm. $\pm$ 0.0005 cm.
4. The rods were vacuum annealed at 900 C. for thirty minutes and cooled.

Upon receipt, the annealed rods were cut into specimen lengths of 4.3 cm. using a carborundum cut-off wheel.

B. CHARACTERIZATION OF FLOW STRESS

Alloy B (see Table 1) was chosen as the representative alloy for this work and was used exclusively. Stress/strain curves were generated in tension on a 4448 N. capacity

Instron testing machine, model 1102 TM-S-L, at a constant strain rate of 0.0127 cm/min. The grips and underslung rig were manufactured at this laboratory. The stainless steel rig shown in Figure 3, was designed to provide for rapid interchange of immersion baths. An anvil, supported in compression by three columns, acted as an extension of the crosshead. The load cell was coupled to the upper grip by means of a reach rod. The underside of the anvil and the base of the lower grip had matched spherical surfaces to permit self-alignment. The reach rod and the upper grip were pin-jointed, and the anvil was slotted to permit rapid installation of the grip assembly into the rig.

The grip assembly is shown in Figure 4. The grips were drilled and tapped to provide a serrated gripping surface and then slit to permit constriction of the specimen when the screws of the collar were tightened.

Strain was measured at the grips using a Bently-Nevada proximeter, model 30B-L18, which was mounted on extension arms to remove it from the immersion baths. The output from the proximeter was fed to a Honeywell Electronik 194 strip chart recorder.

The mechanical compliance of the rig in the range 0 to 4488N. and -196 to 350 C. was determined to be 1.9×10^{-4} cm./N.

Twelve specific temperatures were used in this part of the investigation.

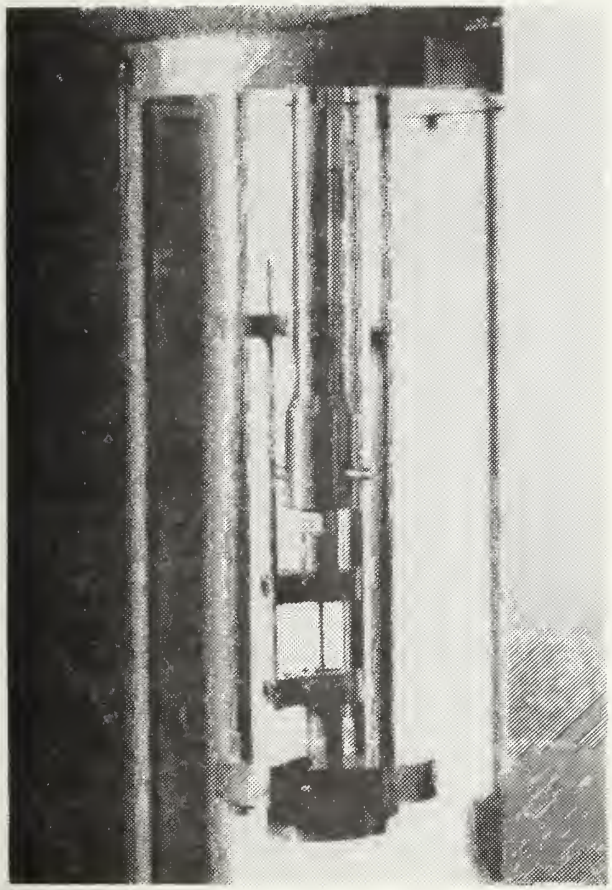

Figure 4

Underslung attachment to Instron machine showing grip assembly in place and pull rod.

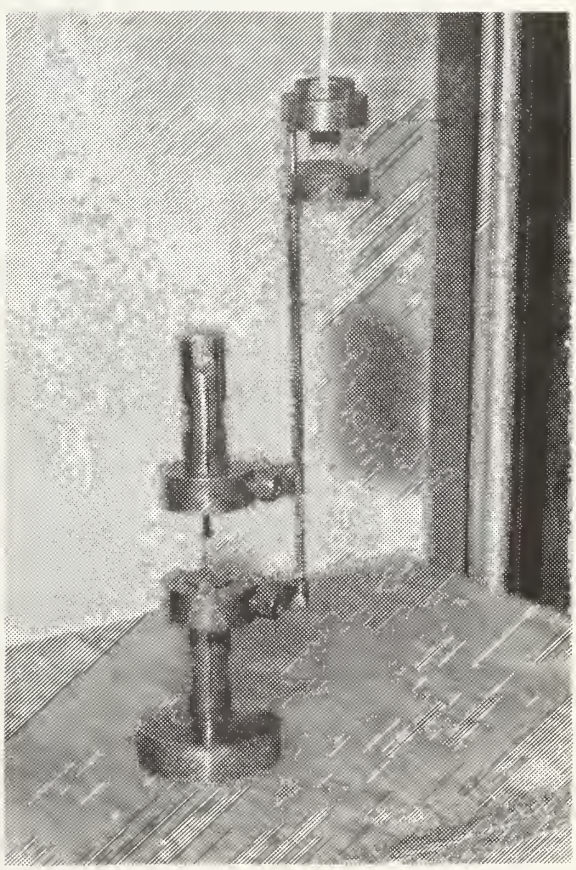

Figure 4

GRIP ASSEMBLY for use with the Instron tensile testing machine, showing proximeter with extension arms.

1. -196 C. Free boiling liquid nitrogen
2. -96 C. Acetone sludge
3. -85 C. Trichloroethylene sludge
4. -23 C. Carbon tetrachloride sludge
5. 0 C. Ice water
6. 23 C. Silicon oil
7. 34 C. Silicon oil
8. 48 C. Silicon oil
9. 92 C. Silicon oil
10. 220 C. Silicon oil
11. 344 C. Potassium nitrate
12. 450 C. Potassium nitrate

Temperature control was maintained in the silicon oil and the potassium nitrate by means of a Honeywell-Brown controller (0 to 1200 C.) with an accuracy of $\pm$ 3 C. Temperature was determined in all cases except liquid nitrogen by means of a Leeds and Northrup millivolt-potentiometer coupled to a chromel/alumel or copper/constantine thermocouple.

The as-annealed specimens were strained to 10% at each of the above temperatures. These data were then corrected for strain rate sensitivity by running a separate test in which the crosshead was stopped at several values of strain and the relaxation recorded. This emperical value of the dynamic portion of the flow stress was then subtracted from the test data to yield a static stress.

C. CHARACTERIZATION OF REVERSION STRESS

Samples of Alloy B were tested in this portion of the investigation. The same test apparatus as described above and shown in Figures 3 and 4 was used except that the output from the proximeter was also fed to a voltage comparator. This voltage comparator was capable of looking at the voltage output from the proximeter and comparing that with any set voltage ($\pm$ 14 volts) to within 0.001 volts. The device, upon comparing the two voltages, would send a signal to activate the extension cycle facility built into the Instron machine, such that a constant strain ($\pm$ 0.05%) would be maintained on the specimen. The thermal response of the rig and machine was thereby negated in the range T<350 C. Above that temperature, the thermal response of the proximeter and its extension arms was such as to invalidate the accuracy of the signal.

The procedure for the characterization of reversion stress was as follows.

1. The specimen was strained at 0.0127 cm./min in silicon oil sludge to a predetermined value. This particular bath was chosen because it allowed for a temperature transition from -60 C to + 220 C. without changing baths.

2. The load was relieved and e_i was recorded. (See Fig. 2)

3. The specimen was constrained at e_i and heated to +200 C., recording the temperature with a copper/constantine thermocouple coupled to a Hewlett Packard 7100B strip chart recorder.
4. The reversion stress was recorded at fixed strain.

Reversion stress tests were also done using alloy C to compare with model tests.

D. CHARACTERIZATION OF THE STABILITY OF REVERSION STRESS

Alloy B was also used in the stress relaxation study, and the same test apparatus was again used. The procedure used follows exactly the first three steps of the procedure to determine reversion stress, as described in part C above, except that the specimen was heated past 200 C. to some predetermined temperature and maintained, recording reversion stress at fixed strain as a function of time. The baths and temperature controllers are those listed in part B above.

E. OBSERVATION OF MODEL TESTS

A 99.9% pure Al_2O_3 tube, as shown in Figure 5, was instrumented internally with four strain gages. The gages were installed by positioning them as desired and then expanding a split concentric tube inside the alumina tube to apply pressure while curing. Two gages were placed axially and two were placed circumferentially.

The nitinol tube shown in Figure 6 was manufactured of alloy C and expanded by Raychem Corporation. It was

FIGURE 5

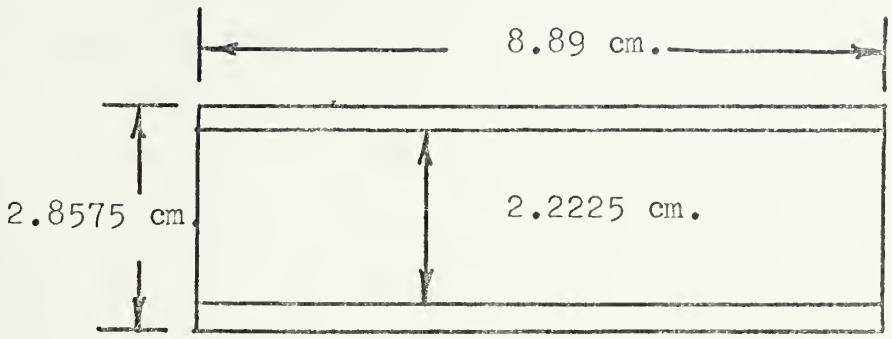

ALUMINA TUBE

FIGURE 6

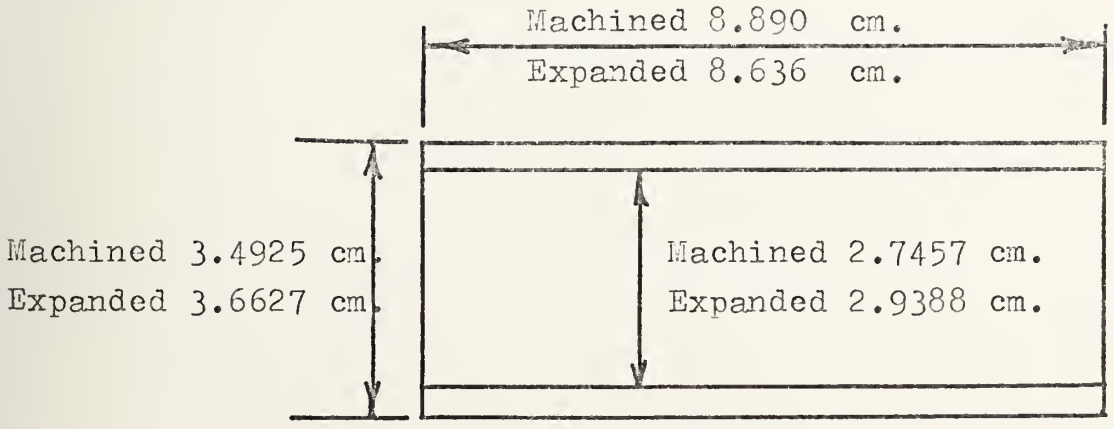

NITINOL TUBE

expanded and maintained in liquid nitrogen.

The alumina tube was placed in the liquid nitrogen bath and inserted into the nitinol tube. The assembly was removed, and the nitinol allowed to revert at room temperature. The assembly was maintained at room temperature for 67 hours and stress was recorded as a function of time.

IV. RESULTS AND DISCUSSION

A. FLOW STRESS

The load/strain/temperature data recorded during the flow stress investigation are shown in Table II. These loads were converted to true stress and corrected for strain rate sensitivity as described above. These corrected true stress values were then plotted against temperature. The values shown in Table III are taken from those curves. They may be illustrated in three ways:

1. Stress/strain curves
2. Stress/temperature curves
3. A three dimensional stress/strain/temperature surface.

There is some value in considering each of the above approaches.

1. Stress/Strain

Five representative stress/strain curves are shown in Figure 7. Similar curves have been reported by Such Ref. D , Pops Ref. J , and many others. It is important to note here that when $T_d > A_f$, the mechanism involved in straining the material is not the same as described for Figure 2. When $T_d > A_f$ the matrix is the high temperature phase instead of thermal martensite, and the mechanism is now $A \rightarrow M(d)$. (Memory in the definition given above cannot occur when $T_d > A_f$ since the reverse transformation, i.e. $M(d) \rightarrow A$, will occur

TABLE II

AS-RECORDED VALUES OF LOAD FOR DETERMINATION OF FLOW STRESS

	STRAIN (%)									
	1	2	3	4	5	6	7	8	9	10
	Newtons									
-196	801	1223	1290	1281	1281	1263	1290	1423	1557	1713
-96	534	672	672	672	672	672	712	845	1112	1379
-86	511	601	601	601	601	601	623	756	934	1156
-22	311	356	336	336	311	311	400	601	845	1112
0	756	807	807	807	807	807	807	807	807	979
23	889	1512	1691	1735	1735	1735	1735	1735	1735	1735
34	889	1512	1757	1779	1799	1846	1890	1913	1946	1957
48	979	1557	1695	1735	1824	1868	1935	1979	2024	2051
92	1023	1592	1601	1650	1779	1868	1957	2046	2113	2180
220	1201	1563	1601	1601	1735	1868	1957	2046	2135	2224
344	1201	1512	1601	1735	1890	2046	2144	2269	2357	2446
450	1290	1467	1579	1735	1845	2046	2144	2269	2357	2446

TABLE III

FLOW STRESS CORRECTED FOR STRAIN RATE SENSITIVITY

TEMP. C.	% STRAIN													
	4		5		6		7		8		9		10	
	MPa	ksi	MPa	ksi	MPa	ksi	MPa	ksi	MPa	ksi	MPa	ksi	MPa	ksi
0	148	21	149	22	151	22	152	22	153	22	155	22	193	28
25	341	49	344	50	347	50	350	51	354	51	357	52	360	52
50	341	49	362	52	373	54	391	57	406	59	417	60	425	62
75	326	47	355	51	373	54	395	57	415	60	428	62	436	63
100	319	46	347	50	373	54	395	57	417	60	436	63	444	64
125	316	46	344	50	373	54	395	57	417	60	440	64	447	65
150	314	45	344	50	373	54	395	57	417	60	440	64	451	65
175	312	45	344	50	373	54	395	57	417	60	440	64	447	65
200	309	45	344	50	373	54	395	57	417	60	436	63	444	64

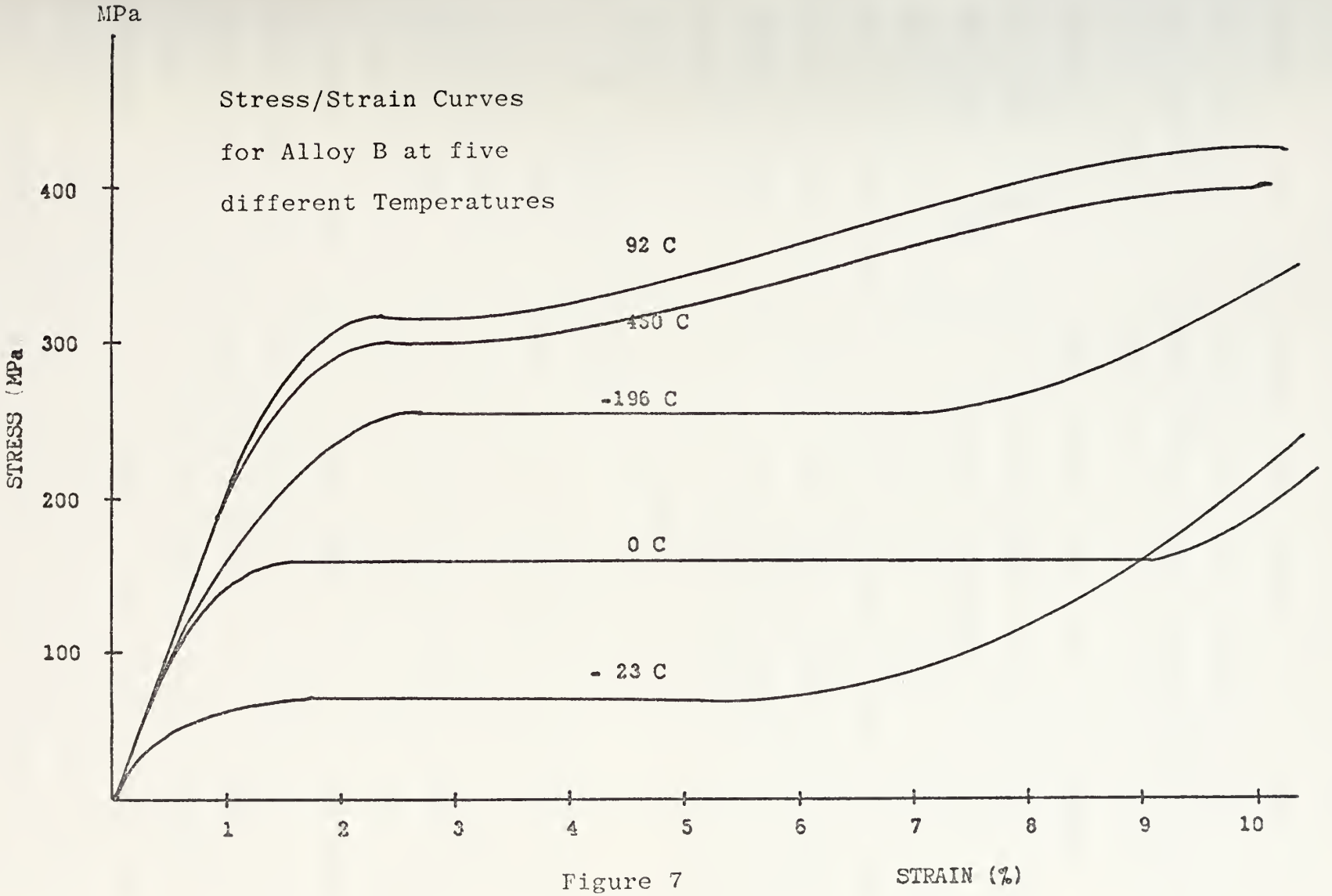
MPa
Stress/Strain Curves
for Alloy B at five
different Temperatures
400
300
200
100
STRESS (MPa
92 C
450 C
-196 C
0 C
- 23 C
1
2
3
4
5
6
7
8
9
10
STRAIN (%)

Figure 7

immediately upon the removal of the stress. For that reason it was not discussed with Figure 2.) On unloading the material, the load does not drop linearly to zero, as the material must undergo the reverse transformation M(d)$\longrightarrow$A. If in a SME material the load is removed prior to D (see Figure 2), all or nearly all of the strain is recovered. Pops [Ref. 9] labeled this mechanism as pseudoelasticity. Wasilewski [Ref. 2] has shown that there is a stress hysteresis (a function of strain) for nitinol. This aspect was not investigated in this project and is mentioned here only to underscore the fact that the stress/strain curves shown in Figure 7 for -23 C. and above represent the reaction A$\longrightarrow$M(d), while the curve for -196 C. represents the reaction M$\longrightarrow$M(d), as described for Figure 2.

2. Stress/Temperature

Curves of stress as a function of temperature at five representative values of strain are shown in Figure 8. Each of these curves may be divided into three regions of temperature as indicated on the figure. In the first region, stress increases or is constant with strain and decreases with temperature. This corresponds to a decrease in the flow stress of the martensitic phase with an increase in temperature, which is in accord with ovserved phenomenon in ordinary materials. It is obvious from Figure 8 that the curve for 10% strain is, in this region, disproportionate, i.e., significant strain hardening occurs between 8% and 10% strain. The implication is that the limit for recoverable

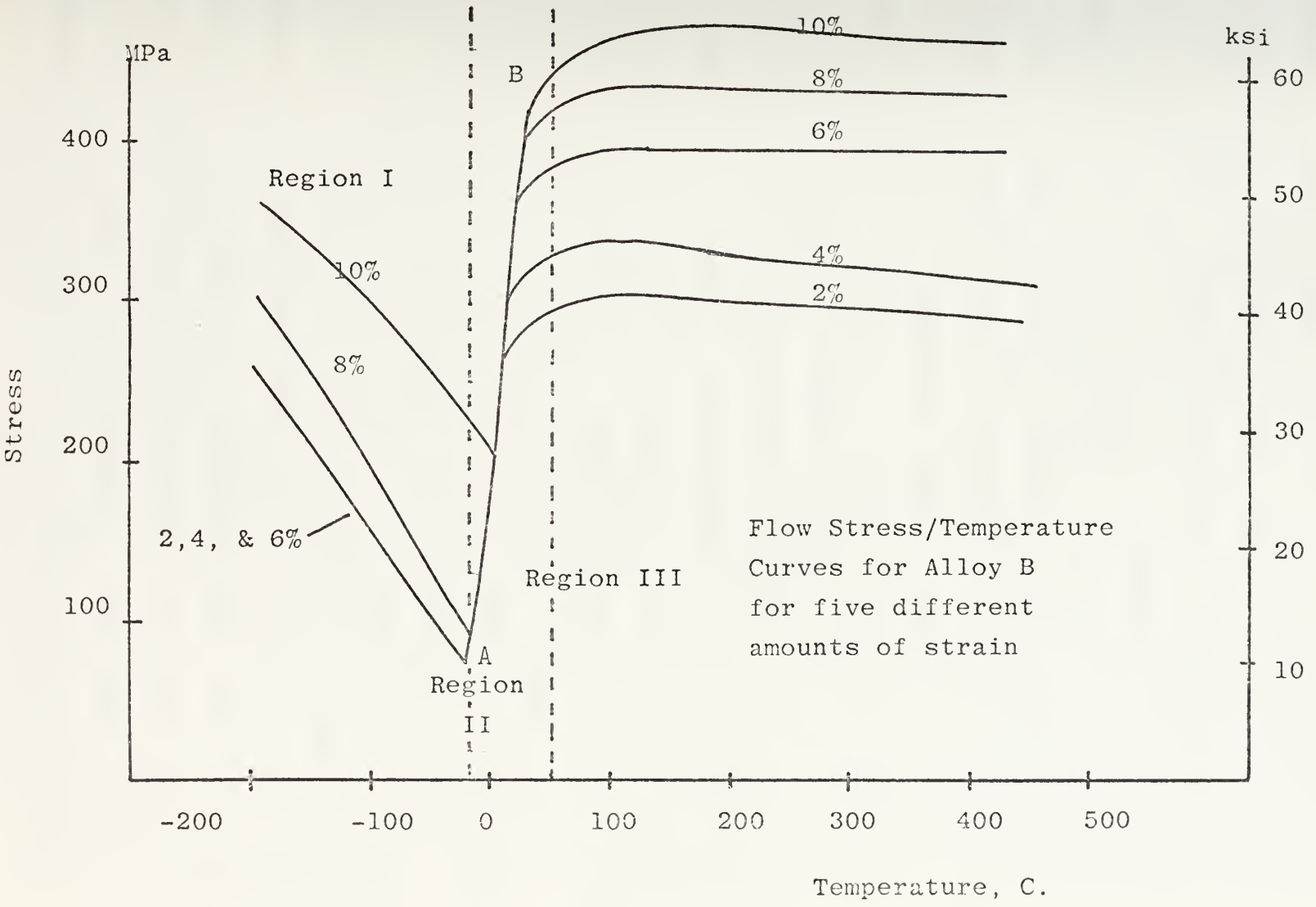
MPa
ksi
Stress
400
300
200
100
60
50
40
30
20
10
Region I
10%
8%
2,4, & 6%
A
B
Region II
Region III
10%
8%
6%
4%
2%
Flow Stress/Temperature Curves for Alloy B for five different amounts of strain
-200
-100
0
100
200
300
400
500
Temperature, C.

Figure 8

strain (point D in Figure 2) is less than 8%, and that strain beyond this point is a result of classical plastic deformation and is irreversible. The exact strain limit is not necessarily obvious from Figure 7; however, Cross, et. al., [Ref. 4] and many others have placed the strain limit between 6% and 8%. Such a conclusion is in accord with the flow stress data shown in region I of Figure 8. The 2% through 6% curve in region I shows a strain independence representative of the plateau on the stress/strain curves from this temperature region. Beyond 6% strain, stress increases rapidly with strain indicating that the $M \longrightarrow M(d)$ is complete at about 6% strain, and that further strain will soon generate dislocations and irreversible deformation. A specimen pre-strained in this region to 8% probably will not have complete recovery, due to this irreversible deformation. Further significance of this will be shown later in relation to reversion stress.

Region II of Figure 8 shows an increase in flow stress with increasing temperature. This corresponds to the above mentioned reaction $A \longrightarrow M(d)$. There are two significant features of this region. The line AB shows a nearly linear variation of stress with temperature. If the line AB were extended to intersect the temperature axis (s=0), it would show a point where the transformation $A \rightarrow M$ would proceed with no applied stress, which defines M_s. The region of point B corresponds to a point where the transformation $A \rightarrow M(d)$ no

longer occurs and the plastic deformation of the high temperature phase begins. Point B, therefore, defines M_d. A line similar to AB has been shown by Krishnan, et. al., [Ref. 10]. For strain values $.02 \leqslant e \leqslant .08$ (the region of most interest for reversion stress), the line AB is common to all curves with the exception of end values, indicating a strain independence. This strain independence in region II indicates that there is very little back stress associated with partial formation of deformation martensite ($A \rightarrow M(d)$) from the high temperature phase. The applied work needed to compensate a positive free energy change above the equilibrium temperature and transform a small volume of material from A to M(d) is a function only of strain at fixed temperature.

Region III shows a decrease in the flow stress with an increase in temperature, and corresponds to a more commonly observed phenomenon wherein an increasing temperature increases the dislocation mobility controlling the deformation of a single phase material. However, the temperature rate of decrease of the flow stress in region III is abnormally low, indicating a continued interaction of the phase transformation with the classical effect of thermally activated dislocation motion.

3. Stress/Strain/Temperature

The three dimensional plot of the flow stress surface (the matrix shown in Table III) is shown in Figure 9.

Figure 9

Three dimension plot of flow stress as a function of strain and temperature for alloy B.

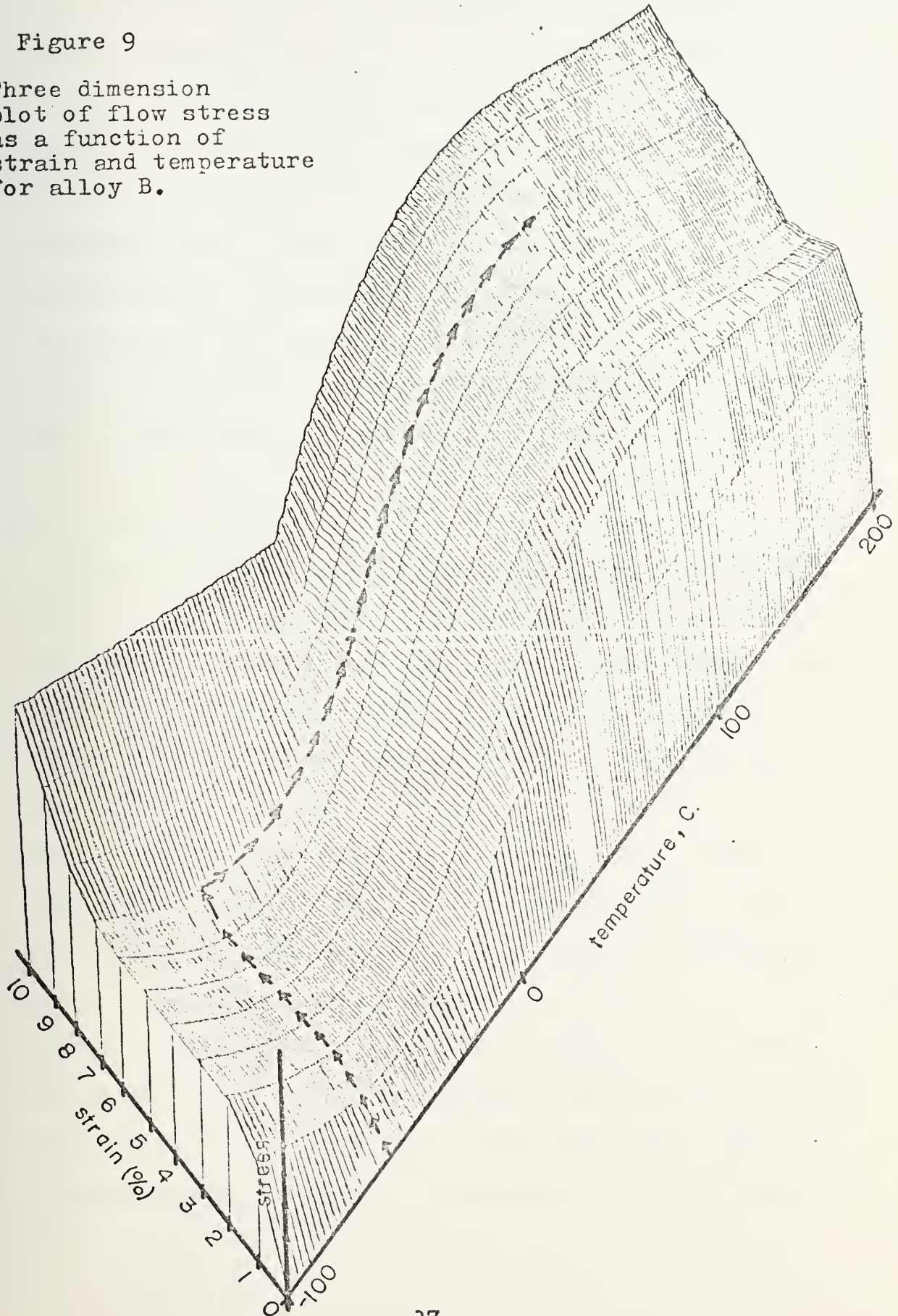

It is presented to support or better exhibit features discussed in the preceeding sections. It is the intent of this study to show that this surface is the limit for reversion stress where the strain axis corresponds to the amount of constrained reversion. More significantly, not only is it the limit, but for the alloy of this study, it is a good approximation to the actual reversion stress at each point. Accordingly, the track on the surface approximates the stress history of a specimen pre-strained at -60 C. to 7% strain and reverted fully constrained to 100 C.

B. REVERSION STRESS

Data collected on reversion stress as a function of pre-strain and subsequent temperature is shown in Table IV. Engineering stresses were converted to true stresses and corrected for thermal strains. The automatic control device on the Instron machine, described above, held the test specimen to a constant deformation, i.e. the engineering strain $(L-L_o/L_o)$ was held constant. For tests involving a temperature change, however, two strains were present. As temperature increased from T_d, the reverse transformation $M(d) \longrightarrow A$ occurred and the specimen attempted to decrease its strain. As it was prevented from doing so, the stress increased. This is, by definition, reversion stress. At the same time the increase in temperature was attempting to increase the length of the specimen; but this was also

TABLE IV

AS-RECORDED VALUES OF REVERSION STRESS

TEMP. C.	% STRESS													
	4		5		6		7		8		9		10	
	MPa	ksi	MPa	ksi	MPa	ksi	MPa	ksi	MPa	ksi	MPa	ksi	MPa	ksi
0	88	13	75	11	88	13	165	24	125	18	44	6	79	11
25	133	19	154	22	140	20	182	26	178	26	86	12	132	19
50	255	37	263	38	277	40	263	38	209	30	206	30	180	26
75	285	41	307	45	329	48	338	49	359	52	338	49	281	41
100	286	42	307	45	329	48	364	53	364	53	366	53	364	53
125	286	42	300	44	325	47	351	51	356	52	355	52	369	53
150	286	42	303	44	324	47	334	48	349	51	342	50	360	52
175	286	42	318	46	322	47	333	48	345	50	323	47	343	50
200	286	42	307	45	321	47	333	48	338	49	312	45	331	48

prevented, causing a decrease in stress. As a practical matter these two effects are inseparable since reversion cannot occur without a temperature increase, and temperature cannot increase without thermal stress or thermal strain. (However, if nitinol is used in a device of composite material as described in section III E, and if the other material or materials has a thermal deformation coefficient which is approximately the same as that for nitinol, then the thermal stress is effectively counteracted.) Nevertheless, in an attempt to better understand the phenomenon of reversion stress, the effects of thermal and reversion stress were analytically separated. This was done by multiplying the thermal strain, as given by Spinner, et. al., [Ref. 11] by the modulus of the flow stress at that value of strain and adding this value to the experimental reversion stress. Table V shows true reversion stress corrected for thermal strain.

A primary goal of this investigation was to demonstrate that the internal stress (reversion stress) is very near in value to the reaction stress developed internally by a sample deformed in a single uniaxial tensile test at fixed temperature. Therefore, data from both types of tests have been corrected so that a comparison could be made between: (1) the applied stress necessary to strain the specimen to a given value of strain, and (2) the

TABLE V

REVERSION STRESS CORRECTED FOR THERMAL STRAINS

TEMP. C.	% STRAIN													
	4		5		6		7		8		9		10	
	MPa	ksi	MPa	ksi	MPa	ksi	MPa	ksi	MPa	ksi	MPa	ksi	MPa	ksi
0	91	13	78	11	93	13	176	26	135	20	48	7	87	13
25	139	20	161	23	149	22	195	28	192	28	93	14	145	21
50	265	39	277	40	293	43	282	41	226	33	225	33	198	29
75	297	43	323	47	349	51	362	53	387	56	369	54	309	45
100	298	43	323	47	349	51	390	57	394	57	400	58	401	58
125	298	44	315	46	345	50	376	55	384	56	388	56	406	59
150	298	44	318	47	344	50	357	52	377	55	374	54	396	58
175	298	44	335	49	342	50	357	52	373	54	352	51	378	55
200	298	44	323	47	340	50	357	52	365	53	340	50	365	53

internal stress developed when a specimen with the same value of strain undergoes the thermoelastic martensitic reversion, all other conditions being equal. Because the strain rate in the reversion tests was experimentally made zero, the flow stress data was corrected to a zero strain rate value. Additionally, the flow stress tests were done at constant temperature, so that it was necessary to correct stress data for thermal strains.

Figure 10 makes a typical comparison between reversion stress and corrected flow stress for alloy B.

Similar plots representing different pre-strains are included as Figures 11-16. These data are not individually discussed, but are included to emphasize the close comparison between reversion stress and corrected flow stress.

The "reversion stress" sample was pre-strained 8% at -60 C. Corrected flow stress at 8% strain and various temperatures is plotted for comparison. A hysteresis in reversion stress as a function of temperature should be expected; i.e., reversion stress resulting from phase transformation is normally dependent on the direction of transformation. The cooling curve represents the transformation $A \longrightarrow M(d)$ while the heating curve represents the reverse transformation $M(d) \rightarrow A$. It is, therefore, reversion stress from the cooling curve which most closely corresponds to corrected flow stress from a uniaxial tensile test on loading ($T_d > A_f$); while the heating curve for

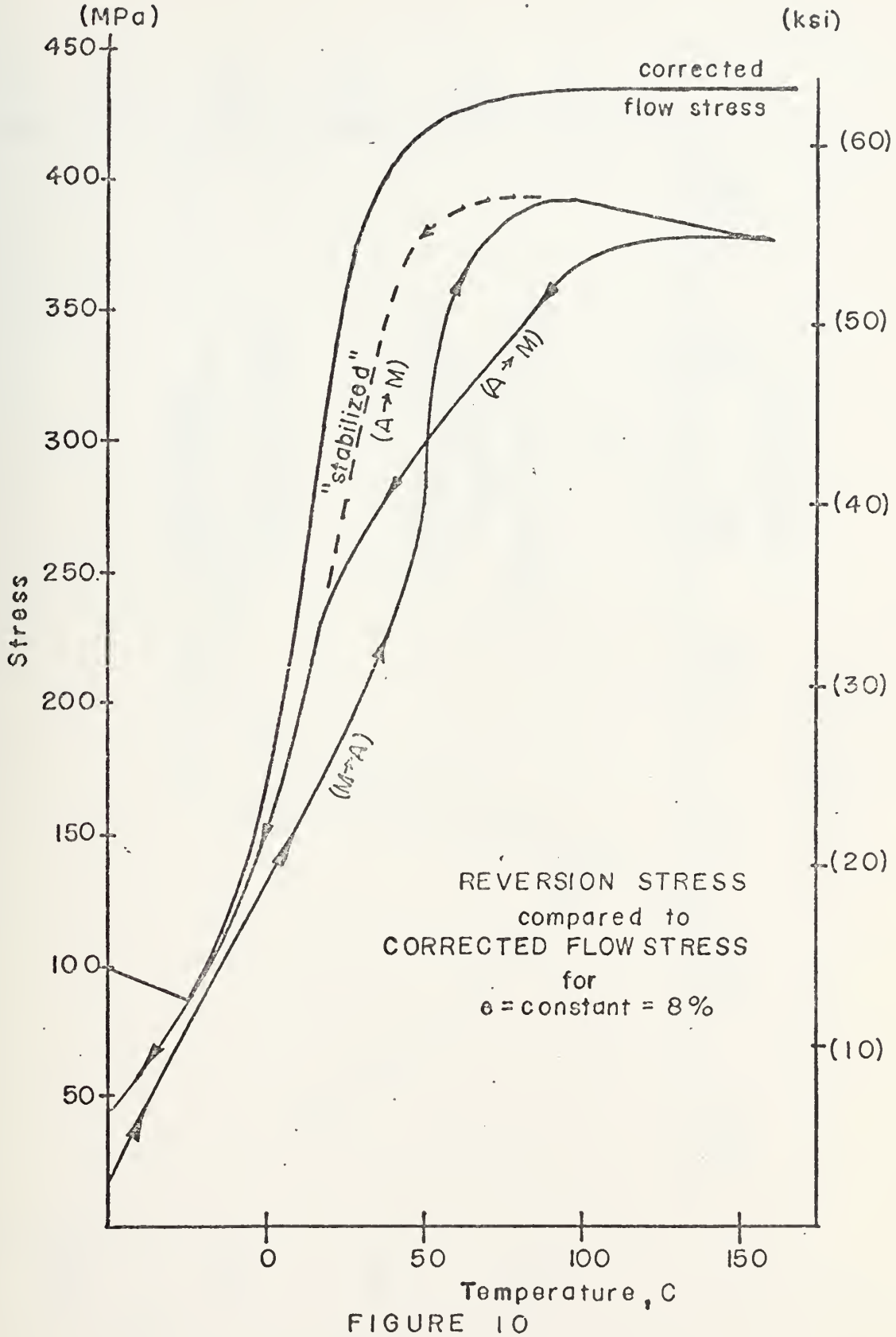
(MPa)
(ksi)
450
400
350
300
250
200
150
100
50
Stress
corrected
flow stress
(60)
(50)
(40)
(30)
(20)
(10)
"stabilized"
(A→M)
(A→M)
(M→A)
REVERSION STRESS
compared to
CORRECTED FLOW STRESS
for
ε = constant = 8%
0
50
100
150
Temperature, C

FIGURE 10

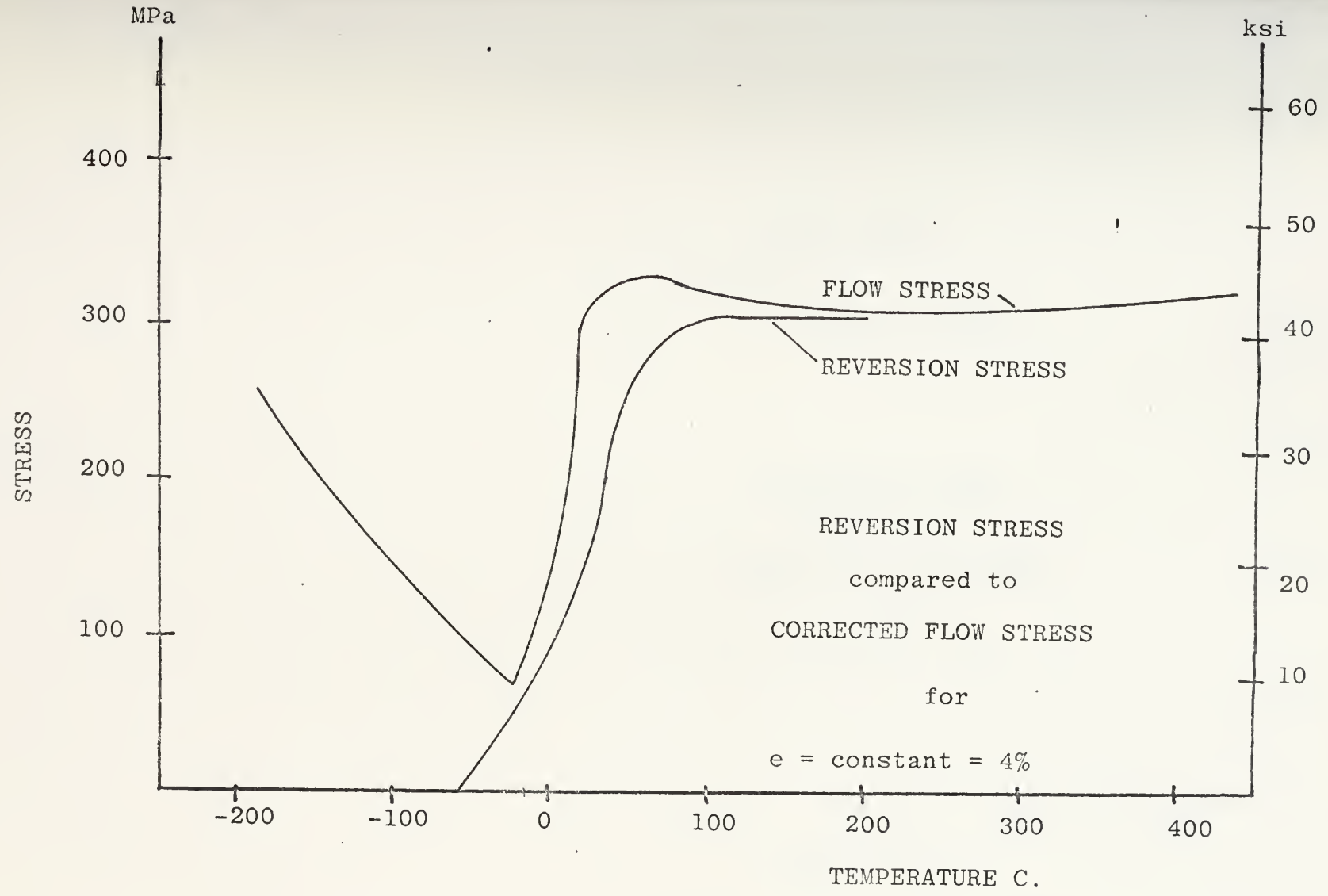
MPa
ksi
400
300
200
100
60
50
40
30
20
10
STRESS
FLOW STRESS
REVERSION STRESS
REVERSION STRESS
compared to
CORRECTED FLOW STRESS
for
e = constant = 4%
-200
-100
0
100
200
300
400
TEMPERATURE C.

Figure 11

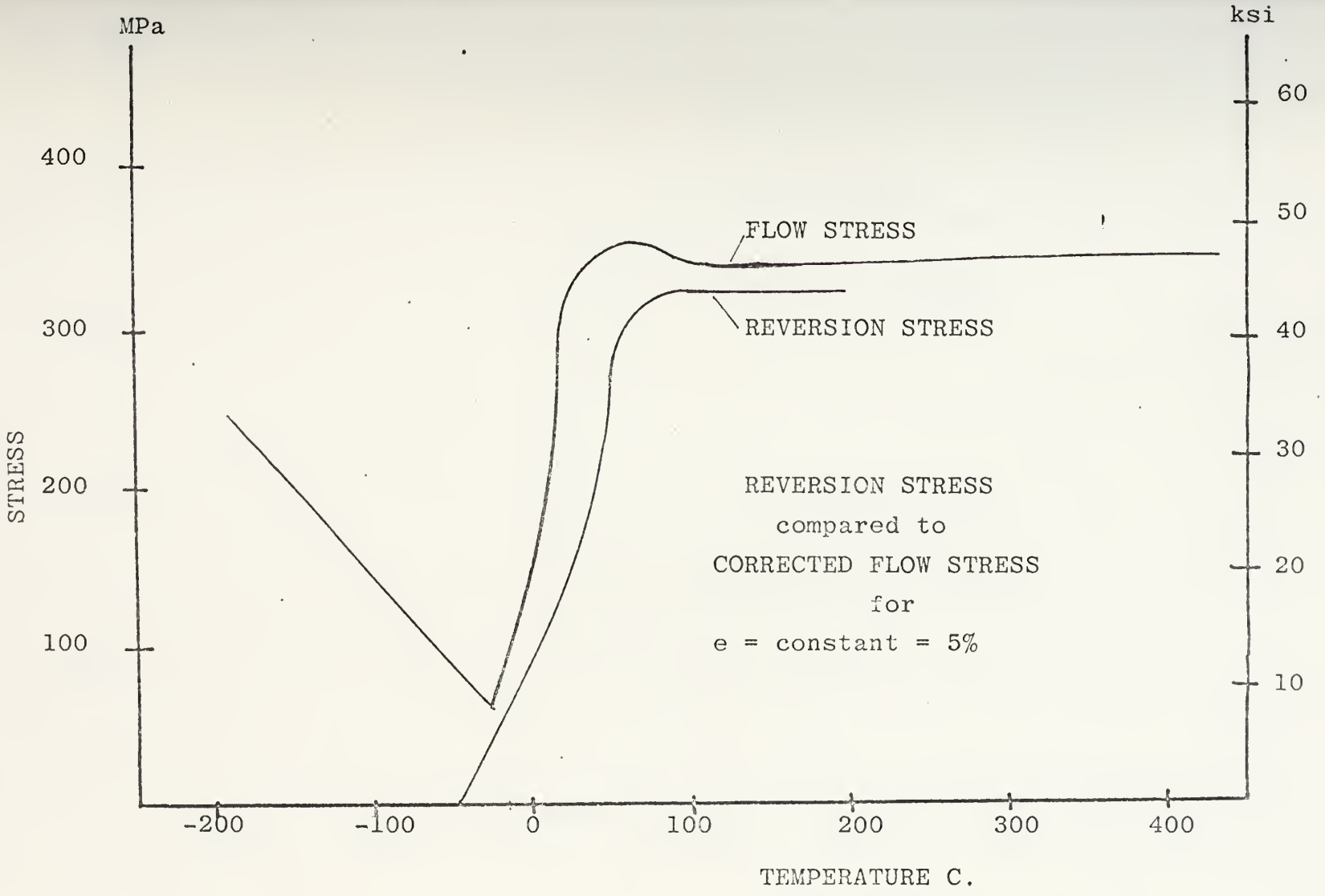
MPa
ksi
400
300
200
100
60
50
40
30
20
10
FLOW STRESS
REVERSION STRESS
REVERSION STRESS
compared to
CORRECTED FLOW STRESS
for
e = constant = 5%
STRESS
-200
-100
0
100
200
300
400
TEMPERATURE C.

Figure 12

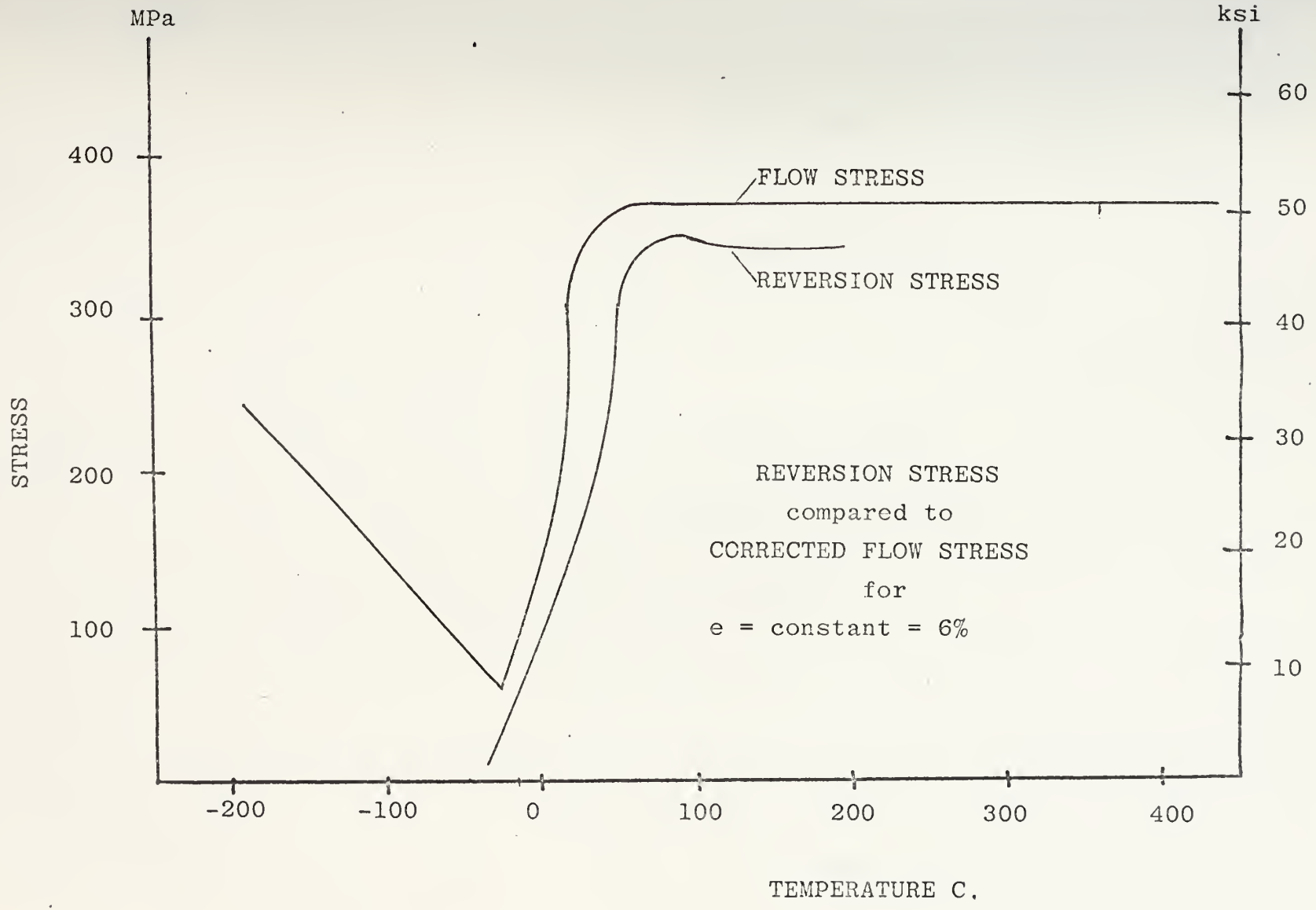
MPa
ksi
400
300
200
100
60
50
40
30
20
10
STRESS
FLOW STRESS
REVERSION STRESS
REVERSION STRESS
compared to
CORRECTED FLOW STRESS
for
e = constant = 6%
-200
-100
0
100
200
300
400
TEMPERATURE C.

Figure 13

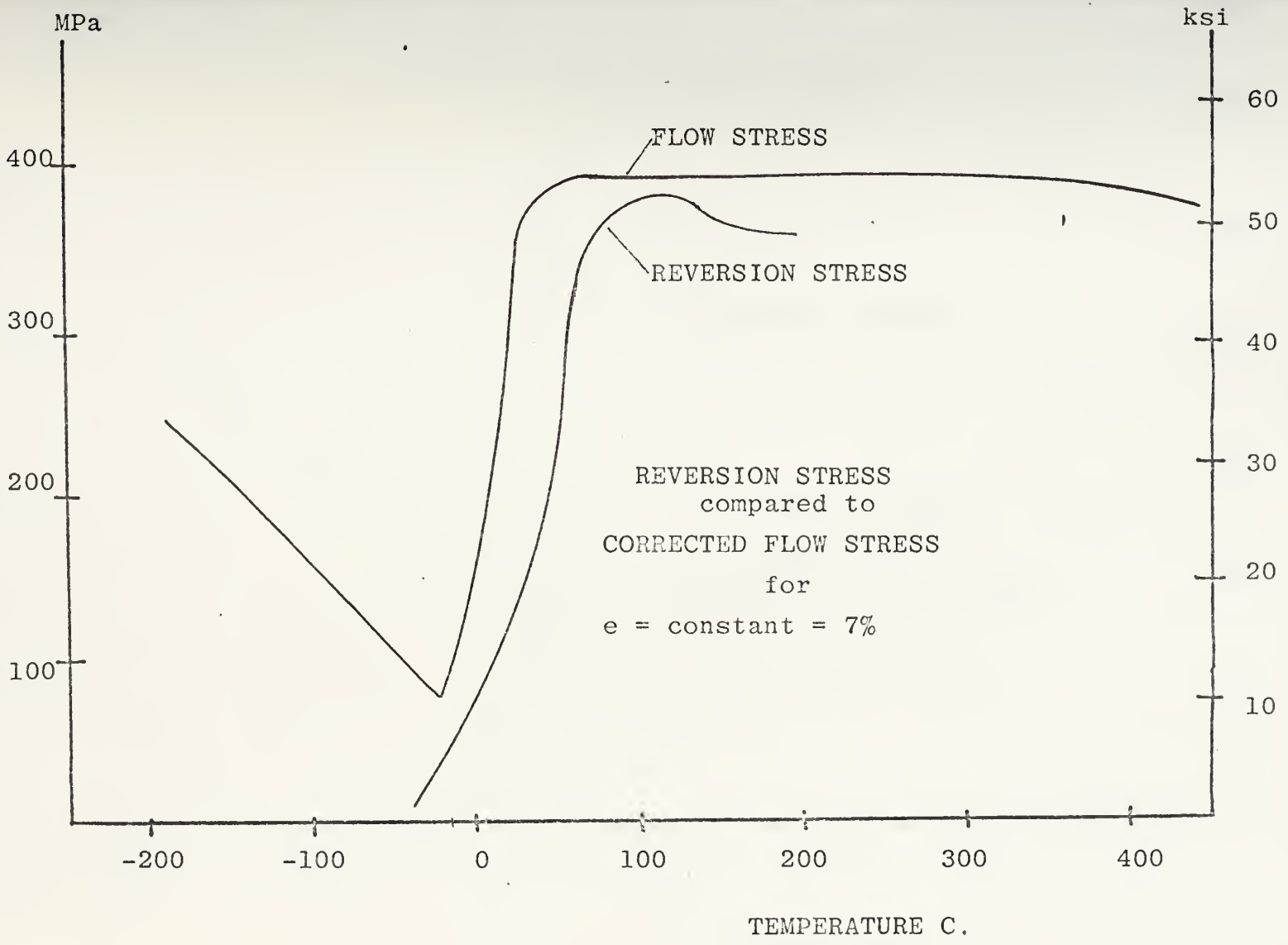
MPa
ksi
STRESS
400
300
200
100
60
50
40
30
20
10
FLOW STRESS
REVERSION STRESS
REVERSION STRESS
compared to
CORRECTED FLOW STRESS
for
e = constant = 7%
-200
-100
0
100
200
300
400
TEMPERATURE C.

Figure 14

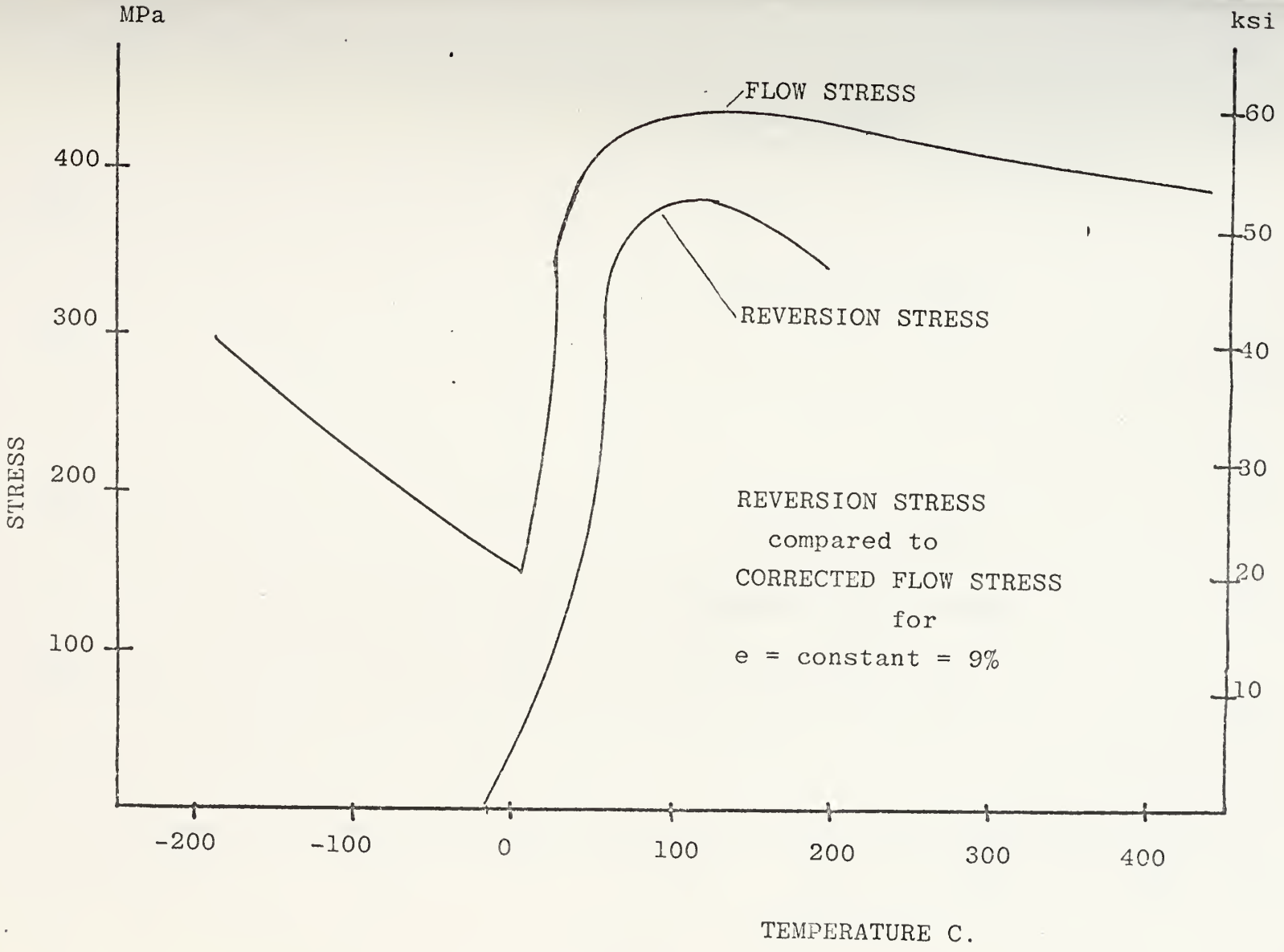
MPa
ksi
FLOW STRESS
REVERSION STRESS
400
300
200
100
60
50
40
30
20
10
STRESS
REVERSION STRESS
compared to
CORRECTED FLOW STRESS
for
e = constant = 9%
-200
-100
0
100
200
300
400
TEMPERATURE C.

Figure 15

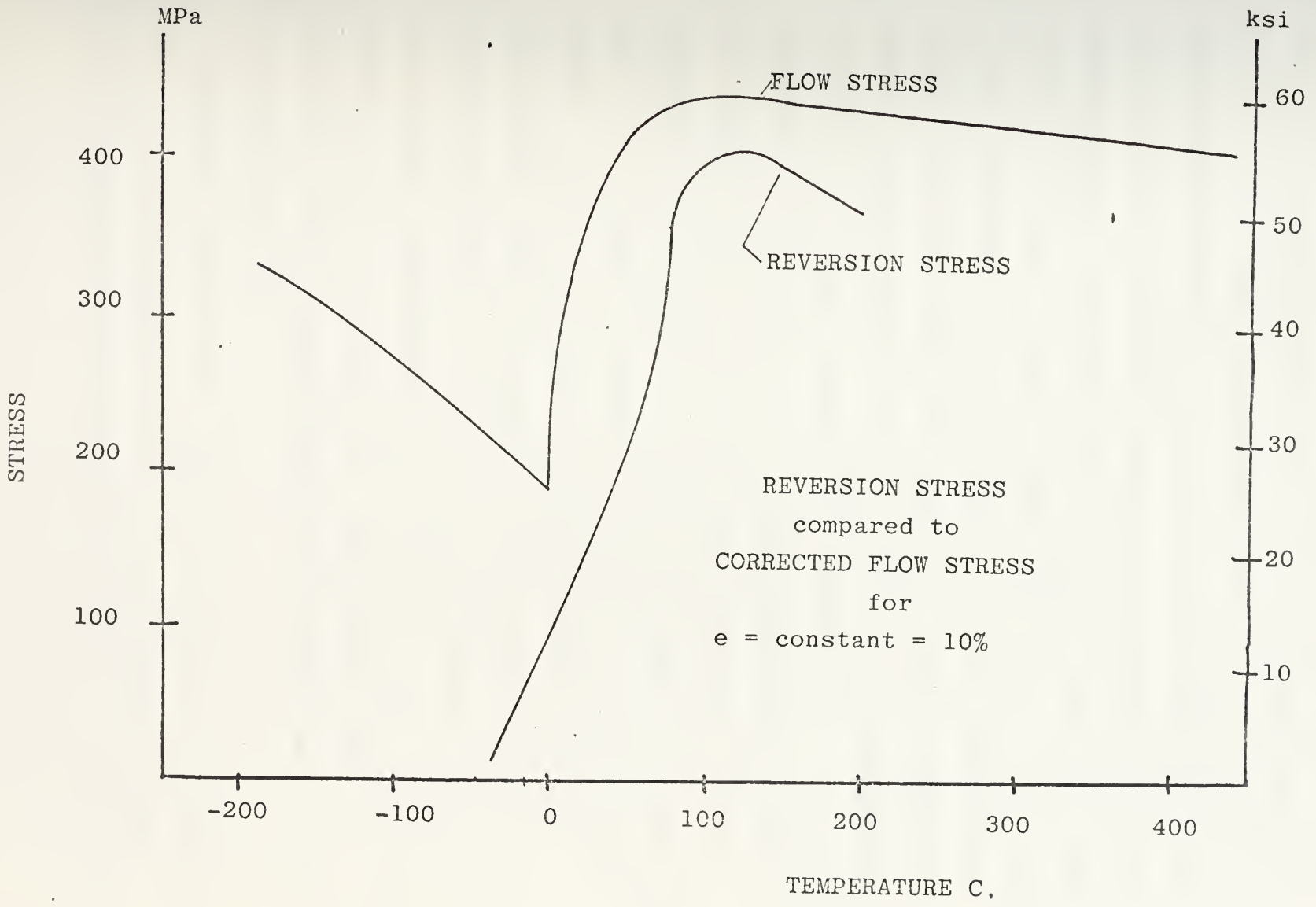
MPa
ksi
FLOW STRESS
REVERSION STRESS
REVERSION STRESS
compared to
CORRECTED FLOW STRESS
for
e = constant = 10%
400
300
200
100
60
50
40
30
20
10
-200
-100
0
100
200
300
400
STRESS
TEMPERATURE C.

Figure 16

reversion stress corresponds to the unloading portion of the stress/strain curve. Beuhring, et. al., [Ref. 12] have shown that at least five thermal cycles ($M_f \leftrightarrow A_f$) are required before a reproducible reversion stress/temperature hysteresis curve is obtained for NiTi. The solid lines of Figure 10 represent data obtained in this investigation, while the dotted portion of the $A \rightarrow M$ curve is from Beuhring, et. al., [Ref. 12] . The cooling portion of the hysteresis curve obtained from this investigation differs initially from the "stabilized" curve, apparently because it was obtained from a specimen which had undergone no strain or thermal cycling prior to the test. A possible explanation can be found by relating experimental work of Allen [Ref. 13] . Allen has found indications that a specimens with no thermal history will initially develop at least three types of martensites, some less stable than others. As the specimen is cycled thermally ($M_f \leftrightarrow A_f$), dislocations begin to accumulate which tend to stabilize a specific martensite. After about five thermal cycles, the more unstable martensites would likely not form on cooling. However, on the first cycle the least stable might be expected to form, thereby reducing the stress level below the stabilized value.

Figure 10 demonstrates that, for alloy B, the reversion stress is closely approximated by corrected flow stress, a fact of practical significance with respect to engineering

design. Thus, optimum pre-strain temperature, maximum reversion stress, and minimum service temperature can readily be determined from simple uniaxial tensile tests at fixed temperature. As a specific example, temperatures above those for the hysteresis curve are required to maintain uniform reversion stress. However, as discussed in section I, the entire curve is easily shifted up or down the temperature scale by alloying procedures. For alloy B, in the region of stable reversion stress, the difference between reversion stress and flow stress is only about 50 MPa (7ksi) so that with full knowledge of this difference, the flow stress could easily be related to design stress while corresponding temperatures could be related to anticipated design temperatures.

Figure 10 shows the reversion stress for 8% pre-strain decreasing slightly with temperature after reaching its maximum value. This stress relaxation with temperature has been found throughout this investigation to be a consistant behavior of samples reverted after pre-strains which exceeded the $M \longrightarrow M(d)$ strain limit of about 6% - 8%, and it appears that slight stress relaxation with temperature above M_d is related to another consistently observed feature, namely, an increase in the temperature transition range with increasing pre-strain. Figure 17 shows the heating portion of four representative reversion stress curves, from the data in Table V. Cross, et. al., [Ref. 4] defined

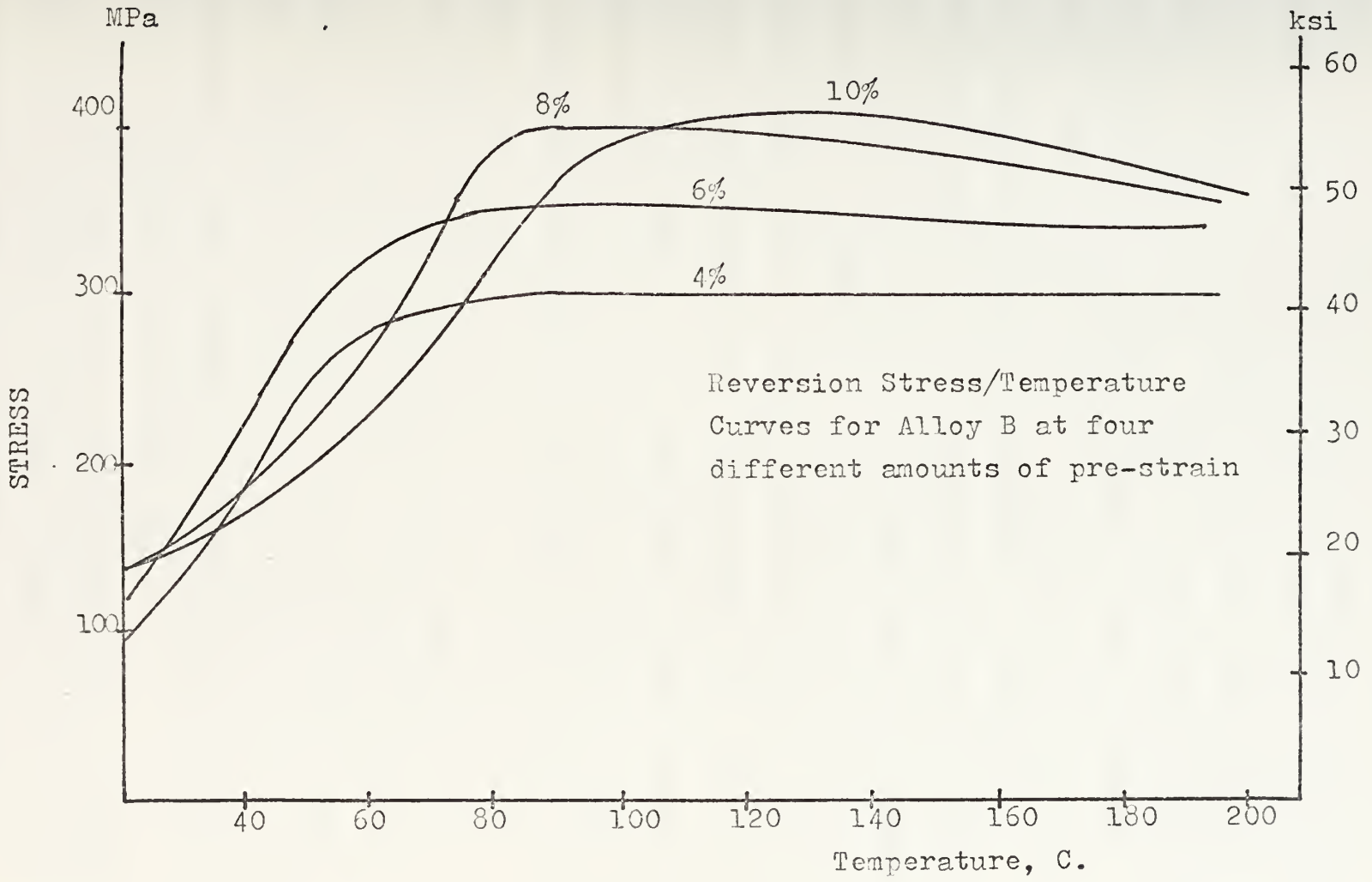
MPa
ksi
STRESS
400
300
200
100
60
50
40
30
20
10
8%
10%
6%
4%
Reversion Stress/Temperature
Curves for Alloy B at four
different amounts of pre-strain
40
60
80
100
120
140
160
180
200
Temperature, C.

Figure 17

the temperature range over which the stress rises rapidly as the "transition"-temperatue range. This temperature range increases with increasing amounts of pre-strain as described above, and as shown in Figure 17. Additionally, the maximum reversion stress increases with increasing amounts of pre-strain. Figure 8 showed that significant strain-hardening occurred between 8% and 10% strain in the low temperature region. Exceeding the strain limit for transforming thermal martensite to deformation martensite results in an increased dislocation density which would have the effect of stabilizing the deformation martensite. Accordingly, the energy required to induce the reversion $M(d) \rightarrow A$ should increase rapidly with increasing pre-strain beyond the strain limit (6% - 8%). Higher temperatures are, in fact, required to revert samples pre-strained beyond the strain limit, as shown in Figure 17. An increased dislocation density may also account for the peak in the reversion stress curve at 10% pre-strain. As this higher density of dislocations accomodates the strain at higher temperatures, a form of stress relaxation is observed when the reversion stress for 10% pre-strain drops below that for 8% in the vicinity of 200 C. This phenomenon is less evident, but nevertheless present, at 8% and is better seen in Figure 10.

The major goal of the experimental work, as stated above, was to compare reversion stress with flow stress as determined from simple uniaxial tensile testing.

Table VI and Figures 10 to 16 show this comparison. In considering these data, a number of factors must be remembered.

1. A more accurate comparison could be made between the reversion stress on cooling and the flow stress on loading as was done in Figure 10, provided the samples were stablized by thermal cycling prior to the reversion test.

2. The large values of stress difference for T=50 C. and below are due to the steep slope of the curves in this region. A small displacement in temperature causes a large displacement in stress as shown in Figure 10.

3. Since, for the most part, the tests were not supported by retesting, the uncertainty shown in Tables VII and VIII may account for a large part of the difference shown in Table VI.

C. STRESS RELAXATION

Although considerable experimental research on the mechanical behavior of NiTi has been done, very little data on the thermal stability of reversion stress is available. Such [Ref. 6] performed a limited investigation of the stability of retained stress. He showed a reduction in stress for alloy A (see Table I) of 13.79 MPa (2ksi) after 20 hours at 377 C. In the present study, seven stress

TABLE VI

DIFFERENCES BETWEEN REVERSION STRESS AND FLOW STRESS

TEMP. C.	% STRAIN													
	4		5		6		7		8		9		10	
	MPa	ksi	MPa	ksi	MPa	ksi	MPa	ksi	MPa	ksi	MPa	ksi	MPa	ksi
0	56	8	71	10	58	8	-24	-3	18	3	107	16	107	16
25	202	29	183	26	198	29	156	23	162	23	264	38	215	31
50	75	11	85	12	80	11	109	16	180	26	192	28	227	33
75	29	4	32	5	24	3	33	5	28	4	60	9	127	18
100	21	3	25	3	24	3	5	1	23	3	36	5	43	6
125	18	2	29	4	28	4	19	2	33	5	52	7	42	6
150	16	2	25	3	29	4	37	5	40	5	66	9	55	8
175	14	1	9	1	31	4	38	5	44	6	88	12	70	10
200	11	1	21	2	32	4	38	5	52	7	96	13	79	11

TABLE VII

UNCERTAINTY IN FLOW STRESS VALUES

TEMP. C.	% STRAIN													
	4		5		6		7		8		9		10	
	MPa	ksi	MPa	ksi	MPa	ksi	MPa	ksi	MPa	ksi	MPa	ksi	MPa	ksi
0	3	1	3	1	3	1	3	1	3	1	3	1	4	1
25	7	1	7	1	7	1	7	1	7	1	7	1	8	1
50	7	1	8	1	8	1	8	1	8	1	9	1	9	1
75	7	1	7	1	8	1	8	1	9	1	9	1	9	1
100	7	1	7	1	8	1	8	1	9	1	9	1	9	1
125	7	1	7	1	8	1	8	1	9	1	9	1	9	1
150	7	1	7	1	8	1	8	1	9	1	9	1	9	1
175	7	1	7	1	8	1	8	1	9	1	9	1	9	1
200	6	1	7	1	8	1	8	1	9	1	9	1	9	1

TABLE VIII

UNCERTAINTY IN REVERSION STRESS VALUES

TEMP. C.	% STRAIN													
	4		5		6		7		8		9		10	
	MPa	ksi	MPa	ksi	MPa	ksi	MPa	ksi	MPa	ksi	MPa	ksi	MPa	ksi
0	2	0	2	0	2	0	4	1	3	1	2	0	1	0
25	3	1	3	1	3	1	4	1	4	1	0	3	3	1
50	5	1	6	1	6	1	6	1	5	1	5	1	4	1
75	6	1	6	1	7	1	7	1	8	1	7	1	6	1
100	6	1	6	1	7	1	8	1	8	1	8	1	8	1
125	6	1	6	1	7	1	8	1	8	1	8	1	8	1
150	6	1	6	1	7	1	7	1	8	1	7	1	8	1
175	6	1	7	1	7	1	7	1	7	1	7	1	8	1
200	6	1	6	1	7	1	7	1	7	1	7	1	7	1

relaxation tests were attempted with alloy B. Two were conducted at 220 C. with specimens pre-strained in liquid nitrogen. The first was pre-stained 5%, the second was pre-strained 8%. In both cases no stress relaxation was observed after 175 hours. Five stress relaxation tests were attempted at 400-450 C. These were done with specimens pre-strained to various amounts of strain (4%-9%). Three were pre-strained in liquid nitrogen and two in silicon oil sludge (-60 C.) Of these, only one relaxed in a classical expodential decay. The inconsistent results of these tests indicated that the experimental procedure may be temperature limited. The proximeter used can become somewhat erratic when subjected to temperatures in excess of 350 C. The conclusion must be that an accurate evaluation of the stability of reversion stress remains to be done, and will require modifications in experimental procedure. It would not, however, be surprising to observe stress relaxation in nitinol at 450 C. as this is .6 T_m (T_m = melting point). The magnitude of the relaxation noted here appears to be excessive in relation to classical stress relaxation. However, the apparently complicated relationship of dislocations to reversion stress could conceivably cause such an anomalous rate of stress relaxation.

D. MODEL TESTS

Monitoring the axial and circumferential stresses generated on the interior wall of an alumina tube by an

outer nitinol sleeve performed the very useful function of demonstrating the validity of characterizing nitinol alloys by employing uniaxial tensile tests. The nitinol sleeve of the model tests was in a triaxial stress state as opposed to the sample tested in uniaxial tension on the Instron machine. Strain was measured, as described in section III E, on the inner wall of the ceramic tube. At this point, the radial stress is zero and the material is effectively in a biaxial stress state. However, knowing the stress at this surface, the principal stresses at any point in the composite body may easily be calculated [Ref. 14]. From those principal stresses, the stress function may be calculated by the Von Mises criterion, i.e.,

$$S = (\tfrac{1}{2}(s_1-s_2)^2 + \tfrac{1}{2}(s_2-s_3)^2 + \tfrac{1}{2}(s_3-s_1)^2)^{\frac{1}{2}}$$ [Ref. 15].

Figure 12 shows the circumferential and axial stress on the outer surface of the nitinol sleeve. (This surface is also free of radial stress, i.e., $s_3 = 0$.) Combining these two values of stress by the Von Mises criterion yields the effective stress, shown in Figure 12 compared with the data from the uniaxial tensile test. While the uniaxial tension test was conducted with the same strain and thermal history as the model, it was constrained absolutely whereas the nitinol in the model deformed the ceramic however slightly and therefore gave up some of its elastic energy, which may explain the lower stress

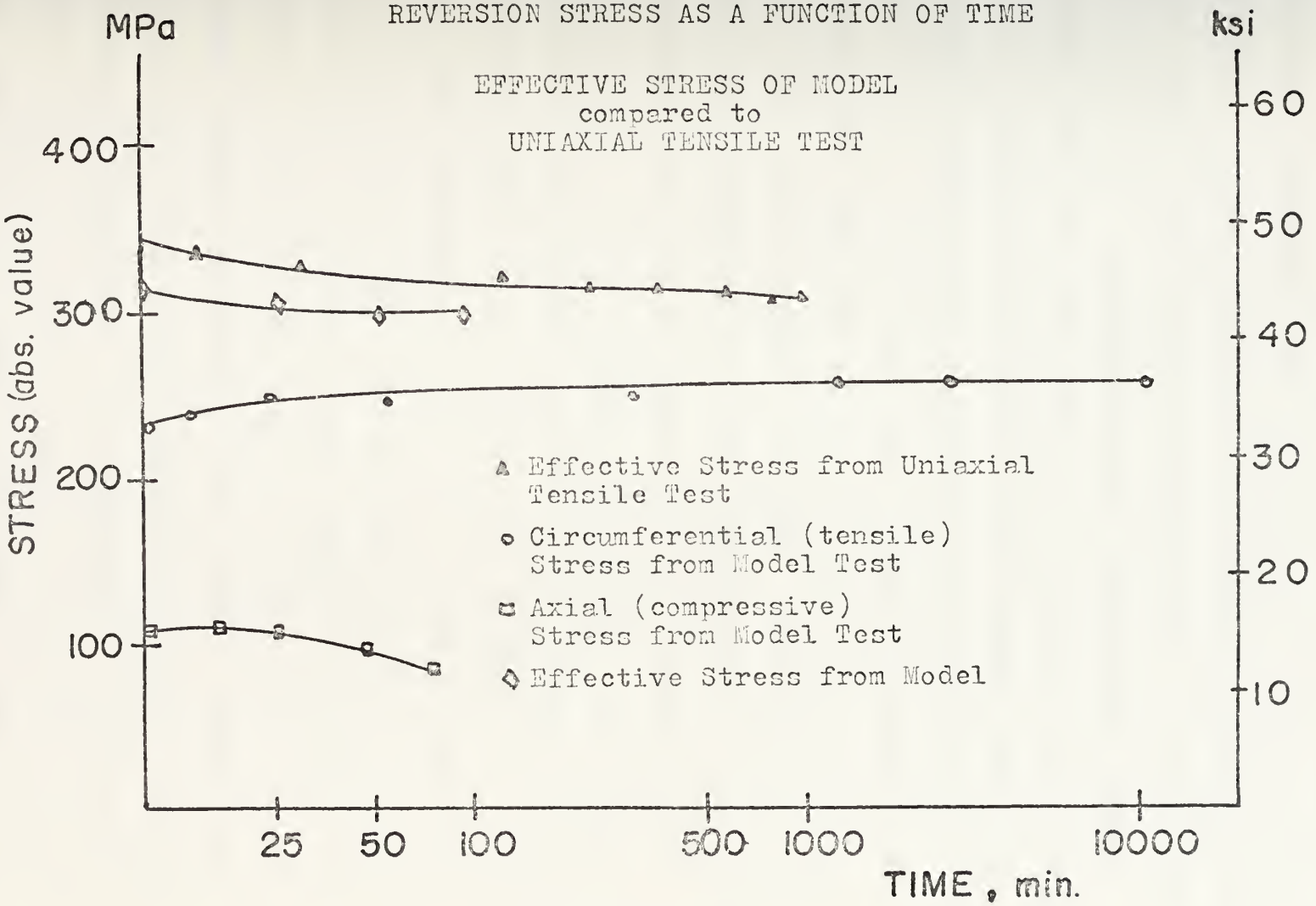
REVERSION STRESS AS A FUNCTION OF TIME
EFFECTIVE STRESS OF MODEL
compared to
UNIAXIAL TENSILE TEST
MPa
ksi
STRESS (abs. value)
400
300
200
100
60
50
40
30
20
10
Effective Stress from Uniaxial Tensile Test
Circumferential (tensile) Stress from Model Test
Axial (compressive) Stress from Model Test
Effective Stress from Model
25
50
100
500
1000
10000
TIME, min.

Figure 18

level for the model. The strain and thermal history of the two tests can be related to Figure 9. Both the uniaxial and model specimens were pre-strained at -196 C. to 8% strain. During this step, they followed the surface along the -196 C. plane to the 8% strain plane. At this point they were both unloaded and they followed the elastic modulus and the -196 isotherm to the base of the figure (s = 0) ending at 7% strain. Upon heating, both moved along the base of the figure and the 7% strain plane until reaching A_s. From there both continued to move up the temperature scale and down the strain scale, still along the base, until reaching 4% strain. At this point they were both constrained and they began moving up the elastic modulus, along the 4% strain plane and increasing in temperature, until reaching the surface. From there, the uniaxial test specimen moved along the surface and the 4% strain plane until reaching room temperature. However, the model specimen, as the level of stress rose, began to deform the ceramic tube and loose some of its own strain. In doing so, it began to fall beneath the surface until reaching a stress level equal to that in the ceramic. The slight increase in stress of the model's circumferential stress may be due to some residual martensite overcoming internal resistance to its transformation during the first 100 minutes, and to heat transfer as the model was more than 400 times as massive as the uniaxial test specimen.

The two strain gages mounted in the axial direction failed within the first hour after the nitinol sleeve was positioned and reverted. The thermal shock of liquid nitrogen undoubtedly contributed to this failure. The relatively low level of axial stress shown in Figure 12 is a result of the fact that the stress is due solely to friction between the nitinol tube and the ceramic tube. The reduction of stress in time is most likely due to slippage rather than to some microstructural phenomenon.

V. SUMMARY AND CONCLUSIONS

1. This study has characterized, for a particular alloy of NiTi, the flow stress as a function of temperture and strain in the range -196 to +450 C. and 0 to 10% strain. Additionally, the reversion stress for the same alloy has been characterized in the range 0 to + 200 C. and 4% to 10% pre-strain. The flow stress, corrected for zero strain rate, has been demonstrated to be an accurate approximation and upper bound for the reversion stress. This close correlation will allow designs utilizing the unique reversion stress developed in nitinol and other SME materials to be based on the more easily generated flow stress data. This correlation appears to be best when the nitinol is pre-strained to its strain limit for recoverable SME (6%-8%). Observed specimens pre-strained beyond the strain limit were unable to maintain their maximum developed reversion stress at high service temperatures, probably because dislocations generated by excessive pre-strain relax at these higher temperatures. This is supported in that specimens pre-strained beyond their strain limit require higher temperatures to accomplish reversion, apparently because dislocations are generated which tend to stablize the deformation martensite.

2. Tests conducted on a model of a possible shipboard application provided evidence of excellent agreement (well within experimental uncertainty) between the effective stress generated in the triaxial stress state of the model and the uniaxial stress developed by simple uniaxial tension tests. The implication here is that a characterization of flow stress for a SME material under consideration for an engineering design can serve as a data base for the reversion stress that may be developed, even in a triaxial application.

3. Nitinol specimens pre-strained at or below the strain limit and maintained at temperatures up to .4 T_m showed no stress relaxation.

4. The intention of the study was to support the use of nitinol as a shipboard material. Alloy B, which was used for the bulk of the testing, is unsuited due to its relatively low yield strength and high transformation temperature. If, however, the properties shown in this study are extrapolated to an alloy such as alloy C, the feasibility of shipboard use is supported, but not verified. There is a continuing requirement for much more study in the area of stress relaxation. Additionally, the model tests, although successful in their goals, need to be supported by re-testing and the reproducibility of results. More elaborate models, even prototypes, need to be built to show conclusively the feasibility of shipboard use.

LIST OF REFERENCES

1. Perkins, J., "Lattice Transformations Related to Unique Mechanical Effects," Metallurgical Transactions, V. 4, p 2709-2721, Dec. 73.

2. Wasilewski, R.J., "The Effects of Applied Stress on the Martensitic Transformation in TiNi," Metallurgical Transactions, V.2, p 2973-2981, Nov. 71.

3. Wayman, C.M., and Shimizu, K., "The Shape Memory ('Marmen') Effect in Alloys," Metal Science Journal, V. 6, p 175-183, 1972.

4. National Aeronautics and Space Administration Report CR-1433, Nitinol Characterization Study, by W.B. Cross, A. H. Kariotis, and F. J. Stimler, Sept. 1969.

5. Tong, H.C., and Wayman, C.M., "Thermodynamic Considerations of Solid State Engines," Metallurgical Transactions, V. 6, p. 29-32, January 1975.

6. Such, C.R., The Characterization of the Reversion Stress for NiTi, M.S. Thesis, Naval Postgraudate School, Monterey, 1974.

7. Tong, H.D., and Wayman, C.M., "Characteristic Temperatures and other Properties of Thermoelastic Martensites," Acta Metallurgica, V. 22, p887-896, July 74.

8. Vinokurov, V.A., and Nikolaev, V.V., "Equipment for Investigating Stress Relaxation at Varying Temperatures," Industrial Laboratory, V.34, p 727-728, May 1968.

9. Pops, H., "Stress Induced Pseudoelasticity in Ternary Cu-Zn Based Beta Prime Phase Alloys," Metallurgical Transactions, V. 1, p 251, January 1970.

10. Krishnan, R.V., Delaey, L., Tass, H., and Warlimont, H., "Thermoplasticity, Pseudoelasticity and the Memory Effects Associated with Martensitic Transformations, Part 2," Journal of Material Science, V.9, p 1536-1544, 1974.

11. Spinner, S., and Rozner, A.G., "Elastic Properties of NiTi as a function of Temperature," Journal of the Acoustic Society of America, V. 40, p 1009-1015, 1966.

12. Battelle Memorial Institute Report, The Effect of Thermal Cycling and Hydrogen Absorption on Selected Properties of 55 Nitinol, by V. F. Beuhring, C.M. Jackson, and H.J. Wagner, Sept. 15, 1969.

13. Allen, R.R., Transmission Electron Microscopic Studies of Shape Memory Reversion Structures in NiTi Alloys, M.S. Thesis, Naval Postgraduate School, Monterey, 1975.

14. Timoshenko, S.P. and Goodier, J.N., Theory of Elasticity, 3rd ed., McGraw-Hill, 1970.

15. Guy, A.G. and Hren, J.J., Elements of Physical Metallurgy, 3rd ed., Addison-Wesley, 1974.

INITIAL DISTRIBUTION LIST

		No. Copies
1.	Defense Documentation Center Cameron Station Alexandria, Virginia 22314	2
2.	Library, Code 0212 Naval Postgraduate School Monterey, California 93940	2
3.	Department Chairman, Code 59 Department of Mechanical Engineering Naval Postgraduate School Monterey, California 93940	2
4.	Assistant Professor Glen Edwards, Code 59 Ed (Thesis Advisor) Department of Mechanical Engineering Naval Postgraduate School Monterey, California 93940	7
5.	Assistant Professor Jeff Perkins, Code 59 Ps (Co-Advisor) Department of Mechanical Engineering Naval Postgraduate School Monterey, California 93940	5
6.	Lt. John M. Johnson, USN R. D. 2 Stoystown, Pennsylvania 15563	1